$\mathbb{Z}_2$ Topological Insulators and The Quantum Spin Hall Effect on Triangular Optical Lattices

by

AHAD KHALEGHI ARDABILI

A Thesis Submitted to the
Graduate School of Sciences and Engineering
in Partial Fulfillment of the Requirements for
the Degree of

Doctor of Philosophy

in

Physics

Koç University

December, 2014

Koç University

Graduate School of Sciences and Engineering

This is to certify that I have examined this copy of a doctoral dissertation by

AHAD KHALEGHI ARDABILI

and have found that it is complete and satisfactory in all respects,
and that any and all revisions required by the final
examining committee have been made.

Chair of Supervisory Committee:

Reading Committee:

Prof. Dr. Tekin Dereli

Prof. Dr. Özgür E. Müstecaplıoğlu

Assoc. Prof. Dr. M. Özgür Oktel

Assis. Prof. Dr. Kaan Güven

Assis. Prof. Dr. Menderes Işkin

Date:

To my Parents

ABSTRACT

In this thesis we studied $\mathbb{Z}_2$ topological insulator and quantum spin Hall effect on triangular optical lattices. In the first part of the study the effect of a strong bichromatic deformation to the $\mathbb{Z}_2$ topological insulator in a fermionic ultracold atomic on triangular lattices. We modified the system proposed by B. Béri and N. R. Cooper, Phys. Rev. Lett. **107**, 145301 (2011) into a dichromatic optical lattice. Large insulating gap of this system allows for examination of strong perturbations. The calculations are done in the nearly free electron limit. We conclude that the $\mathbb{Z}_2$ topological character of the system is robust against a large global perturbation which breaks the inversion symmetry but preserves the time-reversal symmetry.

Then we continue to study the tight binding regime of the system and we compare the band structures and density of states of nearly free electron and tight binding limit.

In Chapter 5, we also propose a tight binding model for the quantum spin Hall system on triangular optical lattices. The proposed Hamiltonian which corresponds to 1/4 magnetic field flux in the case of quantum Hall effect, can be realised using time-periodic driving like lattice shakings. We determine the edge state spectrum which contains gap traversing states as the hallmark of a $\mathbb{Z}_2$ topological insulator.

ÖZET:

Bu tez çalışması üçgen-sel optik ağlar üstünde $\mathbb{Z}_2$-topolojik yalıtkanlar ve kuantumlu spin Hall etkisi üzerinedir. İlk kısımda ultra-soğuk fermiyonik atomlardan oluşan üçgen-sel optik ağlarda $\mathbb{Z}_2$-topolojik yalıtkanların bi-kromatik deformasyonlarının etkisine bakılmıştır. Bunun için B.Beri ve N.R.Cooper [Phys.Rev.Lett.,**107**,145301 (2011)] tarafından önerilen sistem bir bi-kromatik optik ağa genellenmiştir. Sistemin yalıtkan açıklığının büyük olması, büyük pertürbasyonlara bakılmasını olanaklı kılmaktadır. Hesaplar neredeyse serbest elektron limitinde yapılmıştır. Sistemin $\mathbb{Z}_2$-topolojik karakterinin, genel tersinme simetrisini bozan fakat zaman-tersinme simetrisine sahip büyük global pertürbasyonlarla kaybolmayacağı sonucuna varılmıştır.

İkinci kısımda aynı sistem sıkı bağ limitinde incelenmekte ve enerji band yapısı ile durum yoğunluğunun sıkı bağ ve serbest elektron limitleri karşılaştırılmaktadır.

5. kısımda yine üçgen-sel optik ağlarda kuantumlu spin Hall sistemlerinin bir sıkı bağ modeli önerilmektedir. Önerdiğimiz Hamilton operatörünün 1/4 birimlik manyetik akıya karşı gelip zamanda-periyodik bir ağ çalkantısı yoluyla realize edilebileceği gösterilmektedir. $\mathbb{Z}_2$-topolojik yalıtkanlarının belirgin niteliklerinden olan band açıklığını aşabilen durumların varlığı, hesaplanan kenar durum spektrumunda gösterilmektedir.

ACKNOWLEDGMENTS

First and foremost I want to thank my advisor Prof. Dr. Tekin Dereli. I am most grateful and indebted to him for accepting me as Ph.D. student. I want to thank him for his guidance, patience and encouragement during my time here at Koç University. He established my definition of solid and reliable scientific work. Thanks for these fruitful years.

This thesis would not have been possible without Prof. Dr. Müstecaplıoğlu. At a time when I started the topic of topological insulators, he helped me to find a right direction in this research field. His intuitive way of thinking about physics will be an inspiration to me for years to come.

I also want to thank Prof. Dr. Oktel for financial support for the last year of my Ph.D. through TÜBİTAK Project No. 112T974.

I especially thank my parents and my brothers Masood, Behzad and Farzad . My hard-working parents have sacrificed their lives for us and provided unconditional love and care. My love for science has its roots in the way that I've been raised back home. I love them so much, and I would not have made it this far without them. I know I always have my family to count on when times are rough.

I also want to thank my friends at Koç University; Iman Zafarparandeh, Araz Bateni, Sasan Hajizadeh, Enis Doko, Adnan Hasan, Nader Ghazanfari, Ulaş Gökay Seda Ünal and my officemates Yasa Ekşıoğlu, Ozan Sarıyer, Doruk Onal, Murat Öztürk, Deniz Türkpençe, Elif Kağa and in particular my best friends Neslihan Oflaz, Seçil Benli and Neşe Aral who made me feel always at home.

TABLE OF CONTENTS

LIST OF FIGURES

NOMENCLATURE

TR	Time Reversal
TI	Topological Insulator
QHE	Quantum Hall Effect
QSHE	Quantum Spin Hall Effect
TRS	Time Reversal Symmetry
TKNN	Thouless-Kohmoto-Nightingale-den Nijs

Chapter 1

INTRODUCTION

Ginzburg-Landau (G-L) classification of the different phases of matter is based on the various ways of symmetry breaking in the systems. However, there are other way of phase transition possible beyond the usual method of G-L, which is based on the topological characteristic of the system. The Hamiltonian which are homotopic equivalent i.e. those that can change to one another without closing a gap, are known to belong to the same topological family. The corresponding topological phases have certain properties such as the number of gapless edge states and the quantized value of the Hall conductance, which under smooth changes in the material parameters can not be changed, but a quantum phase transition can change these properties.

There are many examples of topological systems with quantum Hall effect and quantum spin Hall effect among them. One of the first examples of the topological insulators is integer quantum Hall effect. The topological characteristic of the IQHE was first formulated by Thouless, *et. al.*in 1982 [2] and the famous TKNN (Thouless, Kohmoto, Nightingale, den Nijs)number was assigned to different IQHE states. The idea is that Chern number which is the integral of Berry curvature of a periodic system under magnetic field over magnetic Brillouin zone gives an integer number. This number which is based on the bulk properties of the system gives the number of edge states. The bulk of IQHE is insulator whereas the edges of the system conduct the current with zero resistance. The quantized current is in the unit of $\sigma_{xy} = \nu e^2/h$ where ν is Chern number. Later Haldane [3] in 1988 showed that IQHE is the consequence of the breaking of time reversal symmetry in the system. He introduced a hexagonal lattice on which the wave function of an electron hopping to its nearest

neighbour acquires no phase while the next nearest neighbour hopping leads to a phase accumulation by electron such as the total flux per a unit cell sum up to zero when the time reversal symmetry (TRS) is broken. This observation shows the significance of TRS and topology in physical systems.

The relation between Landau levels and the velocity dependence of magnetic field in QHE was the motivation for Bernevig and *et. al* [4] to use the spin-orbit coupling which is also velocity dependent to generate QSHE. The idea is that for the QSHE the time reversal must be preserved and one can impose TRS on the QHE by using the concept of spin. If oppositely oriented spins feel the same magnetic field $\vec{B}$ with different signs, then the system can be quantized while preserving TRS. In fact, each spin carry a current multiple of e^2/h but in opposite direction. Kane and Mele in 2005 [5] used a similar idea for graphene which has a hexagonal lattice structure. In fact it can be shown that their model can be reduced to two copies of the Haldane model in which opposite spin directions feel the same magnetic field in opposite directions. Studying various condensed matter problems in cold atomic systems is very important because of the high control over the parameters and an almost impurity free environment. In the thesis we study the method of creating TI in cold atomic systems. Since spin-orbit coupling as the building block of the time reversal invariant TI in condensed matter is an intrinsic character of atoms one needs to create such a force artificially in cold atomic systems. Therefore, the main part of the thesis is about the methods of creating such a force and studying it in two main regimes: nearly free electron limit (NFE) and tight-binding regime (TB).

In this thesis we concluded the $\mathbb{Z}_2$ topological insulators and quantum spin Hall effect on triangular lattices. The first chapter is an introduction to topological insulators. We describe the quantum Hall effect as a topological insulator and explain the relation between the first Chern number and QHE. Later we show how one can go from QHE to quantum spin Hall effect and its relation to the $\mathbb{Z}_2$ topological insulators is given. In the second chapter we explain the atom photon coupling and its relation to optical lattices and the Jaynes-Cumming Hamiltonian is shown.

In the third chapter we review the model proposed by Beri and Cooper [6]. Its tight-binding limit is derived [7]. We compare the band structure and density of states of the model in two regimes; namely the tight-binding and nearly free electron limits respectively. Even if the band gap in tight binding models are not as large as in the case of nearly free electron limit, TIs in ultra cold atomic systems have been studied vastly in the tight binding regime. The optical lattices are described by continuous potentials formed by the combinations of standing waves. It is convenient to treat them as deep potentials.

In the fourth chapter we study [8] the robustness of the topological insulators under a global perturbations. TIs is characteristically keep their properties under local perturbations. Here we look for answering the question: what will happen to such systems under a global change in the system. The bichromatic lattices are mainly used to study localization in the case of incommensurate lattices. Here we first find the band structure changes in the bichromatic case and then in order to find out the topological state of the system we use the method originally given by [5].

In the last chapter, we propose [9] another method for creating an artificial gauge field in cold atomic systems namely, we discuss time-periodic driving like lattice shakings. By applying both DC and AC fields using Raman lasers, we show how one can imprint phases into the atoms so that the Hamiltonian without spin corresponds to accumulation of 1/4 flux magnetic field.

1.1 Introduction to Topological Insulators

1.1.1 Quantum Hall effect

There are different topological insulators which can be classified based on the symmetry they have. We mainly consider the time-reversal topological insulator. In order to follow the pedagogical direction we start with quantum Hall effect (QHE) as a

topological insulators.

In 1982 Thouless *et.al* [2] tried to formulate the quantum Hall effect using Kubo formula, where they found out that the quantized current is due to properties of wave functions. The abstraction on the bundles of wave function over the magnetic Brillouin zone leads to quantization of the current. This bulk properties of an electron gas in a magnetic field has special edge properties. The topological characteristic of the QHE manifests itself in the number of edge states which is a topological number, called the first Chern number. We review the QHE as we use it later on to understand the time reversal invariant topological insulator (TRTI).

The Hamiltonian of non interacting electron gas in a magnetic field $\vec{B}$ can be written as,

$$H = \frac{(\vec{P} - e\vec{A})^2}{2m} + U(x, y), \tag{1.1}$$

where the momentum and gauge potential are in the x-y plane. For a periodic potential,

$$U(x + a, y) = U(x, y + b) = U(x, y). \tag{1.2}$$

Since $\vec{A}$ is not periodic, this Hamiltonian is not invariant under the translation along x- by a and along y- by b. In order to make the system translationally invariant one needs to define new translation operators in the symmetric gauge,

$$\vec{A} = \frac{\vec{B} \times \vec{r}}{2}. \tag{1.3}$$

The periodic Hamiltonian without the vector potential $\vec{A}$ is invariant under the following translation operator

$$T_{\vec{R}} = e^{\frac{i}{\hbar}(\vec{R}\cdot\vec{p})}. \tag{1.4}$$

Now using the symmetric gauge Eq. (1.1) one can introduce a new translation operator,

$$\hat{T}_{\vec{R}} = e^{\frac{i}{\hbar}\vec{R}\cdot[\vec{p}+e\frac{\vec{B}\times\vec{r}}{2}]}. \tag{1.5}$$

Under this new translation operator, the Hamiltonian Eq. (1.1) becomes translationally invariant in the new Brillouin zone which is called magnetic Brillouin zone. The

new translation operators do not commut with each other,

$$\hat{T}_a\hat{T}_b = e^{2\pi i\frac{eB}{h}ab}\hat{T}_b\hat{T}_a, \tag{1.6}$$

when the magnetic flux $eB/hab = p/q$ where q is integer, one can define an enlarged unit cell which is called the magnetic unit cell with the Bravais lattice,

$$\vec{R} = n(q\vec{a}) + m\vec{b}. \tag{1.7}$$

The corresponding Brillouin zone is called magnetic Brillouin zone with the following vectors,

$$\vec{k}_1 = (\frac{2\pi}{qa}, 0), \tag{1.8}$$

$$\vec{k}_2 = (0, \frac{2\pi}{b}). \tag{1.9}$$

The current of the quantum Hall system is quantized in multiples of unit e^2/h. The Laughlin explanation of the quantisation of current which is enlightening is given here. One can imagine a metal ribbon sheet which is bent into a loop of circumference L and is pierced with a perpendicular magnetic field $\vec{B}$. In order to relate the potential drop between two edges V to the current carried around the loop one can differentiate the total energy of electron gas with respect to vector potential $\vec{A}$. The derivative is non zero for extended wave functions. If all the states are localised the only change would be a phase difference $\mathrm{e}^{iex\vec{A}/\hbar c}$. If the states would be extended then the phase changes must come in discrete manner to retrieve the single valuedness condition of the wave function,

$$\vec{A} = n\frac{hc}{eL}. \tag{1.10}$$

Then one needs to consider the energy difference due to addition of one flux unit $\Delta\phi = hc/e$ to system, which we know to bring the system back to itself. The energy increases by the transferr of n electron from one edge to other and therefore the current becomes

$$I = c\frac{neV}{\Delta\phi} = \frac{ne^2V}{h}. \tag{1.11}$$

In order to show how this quantization is related to topology, we review here the method given by Kohmoto [10]. The generalised Bloch functions for the magnetic Brillouin zone can be written as,

$$u^{\alpha}_{k_x k_y}(x+qa,y) = e^{\frac{-i\pi py}{b}} u^{\alpha}_{k_x k_y}(x,y), \tag{1.12}$$

$$u^{\alpha}_{k_x k_y}(x,y+b) = e^{\frac{i\pi px}{qa}} u^{\alpha}_{k_x k_x}(x,y). \tag{1.13}$$

Here α refers to band index and wave function is written in the Bloch form :

$$\psi^{\alpha}_{k_x k_y} = e^{i(k_x x + k_y y)} u^{\alpha}_{k_x k_y}(x,y). \tag{1.14}$$

Since we are interested in the Hall current, (*i.e.* the linear response of current in the perpendicular direction to the applied electric field) we use the celebrated Kubo formula in the limit of zero temperature and zero frequency (static limit):

$$\frac{e^2\hbar}{i} \sum_{E_\alpha < E_F < E\beta} \frac{v_{y\alpha\beta}v_{x\beta\alpha} - v_{x\alpha\beta}v_{y\beta\alpha}}{(E^\alpha - E^\beta)^2} \tag{1.15}$$

where

$$v_{x\alpha\beta} = \frac{1}{\hbar}\langle\alpha|\frac{\partial H}{\partial k_x}|\beta\rangle, \tag{1.16}$$

$$v_{y\alpha\beta} = \frac{1}{\hbar}\langle\alpha|\frac{\partial H}{\partial k_y}|\beta\rangle. \tag{1.17}$$

By working out the above formula one can derive the following Hall current,

$$\sigma^{\alpha}_{xy} = \frac{e^2}{h}\frac{1}{2\pi i}\int d^2k[\vec{\nabla}_k \times \hat{A}(k_x,k_y)]_z, \tag{1.18}$$

where

$$\vec{A}(k_x k_y) = \int d^2r u^*_{k_x k_y}\vec{\nabla}_k u^*_{k_x k_y}. \tag{1.19}$$

If $\vec{A}$ is defined over a torus and if it is uniquely defined, then applying the Stokes theorem we find $\sigma^{\alpha}_{xy} = 0$. But $\vec{A}$ is defined as the derivative of wave functions and the wave function of the Hamiltonian (1.1) is zero in some points inside the magnetic Brillouin zone. Therefore there will exist a singularity so that $\sigma^{\alpha}_{xy} \neq 0$. A torus can be covered by four neighbourhoods, N_i, $i = 1, ..., 4$ and the wave function can be taken

as the sections in the fiber of the principal $U(1)$ bundle. A principal $U(1)$ bundle is a topological space which is locally isomorphic to $N_i \times U(1)$ in each neighbourhood of N_i. Despite the fact that a global phase can not be defined for the wave functions of the Eq. 1.1 which is non zero every where one can define in each patch N_i a smooth global phase $e^{i\theta^i(x,y)} = u_{k_x k_y}/|u_{k_x k_y}|$ where i refers to patch index. Then we can define a transition function

$$\phi_{ij} = e^{i(\theta^i - \theta^j)}. \tag{1.20}$$

After the construction of non trivial fiber bundle, one can find the classification of fiber bundles which are based on the transition characterisation. The integers which characterise the fiber bundle classes are the integral that involves the curvature of the fibers. One can write the corresponding connection 1-form as

$$\omega = g^{-1}Ag + g^{-1}dg, \tag{1.21}$$

where $g \in U(1)$ and

$$A(k_x, k_y) = \hat{A}_\mu(k_x, k_y)dk_\mu = \langle u_{k_x,k_y}|\partial_\mu|u_{k_x,k_y}\rangle. \tag{1.22}$$

Now since we have connection we can find the corresponding curvature 2-form,

$$F = dA = \partial_\nu \hat{A}_\mu dk_\mu \wedge dk_\nu, \tag{1.23}$$

which is the first Chern form $c_1 = i/2\pi F$. The integration of the first Chern form over a closed manifold which is torus T^2, we find the first Chern number

$$C_1 = \frac{i}{2\pi}\int F = \frac{i}{2\pi}\int dA = \frac{i}{2\pi}\partial_\nu \hat{A}_\mu dk_\mu \wedge dk_\nu, \tag{1.24}$$

that is an integer [11]. This number is integer regardless of any particular connection chosen. A comparison of the equations (1.24) and (1.18) shows that

$$\sigma^\alpha = -\frac{e^2}{h}C_1. \tag{1.25}$$

Here σ is Hall conductivity of each filled band which is an integer number.

1.1.2 Quantum Hall effect with broken time reversal symmetry

QHE is perceived as the creation of the Landau levels in the presence of a uniform external magnetic field. However, in order to create QHE one needs to break the time reversal symmetry [3]. In the Haldane model the time reversal symmetry is broken without any external magnetic field (*i.e.*, magnetic ordering) so that the net magnetic flux through a unit cell of the hexagonal lattice is zero. The tight-binding Hamiltonian has nearest neighbour hopping parameter t_1 and second-neighbour sites hopp by the parameter t_2. Since the net flux through unit cell vanishes, one can choose a periodic vector potential $\vec{A}\,(\vec{r})$. Therefore the hopping parameters get the phase

$$e^{i\frac{e}{\hbar}\int \vec{A}\cdot d\vec{r}}, \tag{1.26}$$

The integral is taken along the hopping path. As one goes around a unit cell, the phase accumulated by the first-neighbour sums up to zero. The t_2 matrix on the other hand get a phase ϕ.

$$H = \sum_{<i,j>} t_1 a^{\dagger}_{\vec{i}} b_{\vec{j}} + \sum_{\ll \vec{i},\vec{j} \gg} t_2 e^{i\phi_{\vec{i},\vec{j}}} (a^{\dagger}_{\vec{i}} a_{\vec{j}} + b^{\dagger}_{\vec{i}} b_{\vec{j}}), \tag{1.27}$$

where $\phi_{\vec{i},\vec{j}}$ is the phase between two next nearest neighbour and we have two sub lattices that we show them by A and B Fig. 1.1 with creation operator$a$ and annihilation operator $a^{\dagger}$.

The Fourier transformation of the above Hamiltonian is given by,

$$H(\vec{k}) = \sum_i 2t_2 \cos(\phi) \cos(\vec{k}\cdot\vec{b}_i)\mathbb{1} + t_1 \Big(\cos(\vec{k}\cdot\vec{a}_i)\sigma_x + \sin(\vec{k}\cdot\vec{a}_i)\sigma_y\Big) - 2t_2 \sin(\phi) \sin(\vec{k}\cdot\vec{b}_i)\sigma_z, \tag{1.28}$$

where σ_i are Pauli matrices, $\vec{a}_i$'s are the displacement from a B site to its three nearest neighbours and

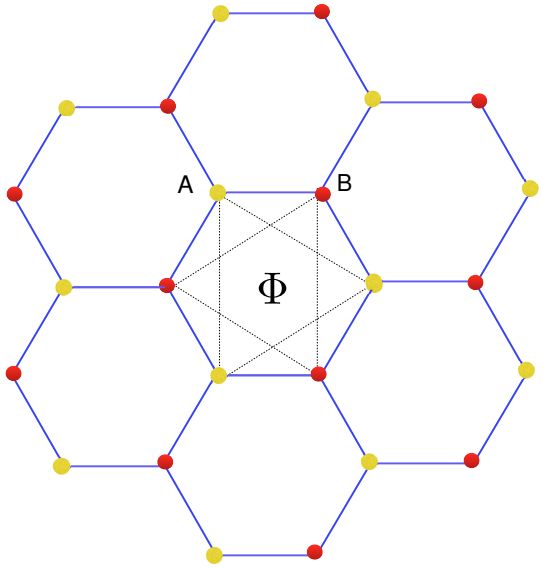

Figure 1.1: The configuration of a hexagonal lattice which is introduced by Haldane. The net flux through the unit cell is zero while the next nearest neighbour hopping acquire a phase. The A and B which are shown in yellow and red colour refer to A and B sub lattices.

$$\vec{b}_1 = \vec{a}_2 - \vec{a}_3, \tag{1.29}$$

$$\vec{b}_2 = \vec{a}_3 - \vec{a}_1, \tag{1.30}$$

$$\vec{b}_3 = \vec{a}_2 - \vec{a}_1. \tag{1.31}$$

Diagonalization of Eq. 1.28 leads to,

$$E = H_0 \pm \sqrt{H_1^2 + H_2^2 + H_3^2}, \tag{1.32}$$

where

$$H_0 = \sum_i 2t_2 \cos(\phi) \cos(\vec{k} \cdot \vec{b}_i), \tag{1.33}$$

$$H_1 = \sum_i t_1 \cos(\vec{k} \cdot \vec{a}_i), \tag{1.34}$$

$$H_2 = \sum_i t_1 \sin(\vec{k} \cdot \vec{a}_i), \tag{1.35}$$

$$H_3 = \sum_i 2t_2 \sin(\phi) \sin(\vec{k} \cdot \vec{b}_i). \tag{1.36}$$

When $t_2 = 0$ the system becomes degenerate at two corners of the Brillouin zone since H_1 and H_2 are zero at $K = (4\pi/3\sqrt{3}a, 0)$ and $K' = (-4\pi/3\sqrt{3}a, 0)$ where a is the lattice constant. But when the next nearest neighbour hopping are present, the gaps open at the corners $\vec{K}$ and $\vec{K}'$. If now one calculates the Chern number, it turns out that the Chern number is either $+1$ or -1 depending on the sign of ϕ.

1.1.3 Quantum spin Hall effect as two copies of quantum Hall effect

The idea of the previous chapter that time reversal symmetry is the essence of QHE has later on became useful in the context of quantum spin Hall effect. The intrinsic spin Hall effect is the result of spin-orbit coupling in semiconductors [4]. The observation of possible dissipationless spin current is due to the applied electric field and the resulting current is time reversal invariant raise thus the question of the possible existence of a quantized current like QHE [4]. The role played by the magnetic field can be shown by studying the spin-orbit coupling (SOC). Spin orbit coupling is velocity dependent and can be written as

$$(\vec{p} \times \vec{E}).\vec{\sigma}, \tag{1.37}$$

where $\vec{E}$ is the electric field and σ's are Pauli matrices. Unlike the magnetic field, the electric field doesn't break the time reversal symmetry. If the momentum of the particle is confined to xy- plane and the electric field components are in the same plane, then the above equation becomes

$$(E_x p_y - E_y p_x)\sigma_z. \tag{1.38}$$

This term in the Hamiltonian implies that a particle with spins opposite in directions experiences opposite magnetic fields. This idea as we will show later is also used by Kane and Mele [5] in their seminal paper where they discuss the mirror symmetric spin-orbit coupling as the generalised version of the Haldane model. However, since an electric field configuration such as Eq. (1.38) is not easy to implement they proposed to study the effect in the context of semiconductors. They considered zinc-blend semiconductors under strain which can be described by a Hamiltonian with spin-orbit coupling of the form Eq. 1.38.

1.2 Classification of Topological Insulators

There are several types of topological insulators, which are distinct due to the different symmetries that they have. Here we review the classification method given in [12] The TI Hamiltonian of a gapped non-interacting system of fermions can be characterised by making the use of the one to one correspondence between single-particle Hamiltonian and symmetric spaces which are classified by Cartan. The topological insulators are different from a trivial insulator due to the existence of metallic edge states which can not be deformed continuously to a trivial insulator. The ten fold classification of single particle Hamiltonian is given in table 1.2. Since we are interested in AII class that host a time-reversal invariant $\mathbb{Z}_2$ topological insulator, we review the idea of classifying for this special group, but the same method can be applied to other classes as well. The key symmetry here is time reversal symmetry which makes the eigen-states of the system doubly degenerate, known as Kramers degeneracy. Therefore we use the following notation for the states that span the Hilbert space,

$$|1\rangle, \theta|1\rangle, |2\rangle, \theta|2\rangle, ... \tag{1.39}$$

The time reversal operator is given by

$$\theta = UK, \tag{1.40}$$

Cartan label	T	C	S	Hamiltonian
A (unitary)	0	0	0	U(N)
AI (orthogonal)	1	0	0	U(N) / O(N)
AII (symplectic)	-1	0	0	U(2N)/ Sp(2N)
AIII (chiral unitary)	0	0	1	U(N+M)/U(N)× U(M)
BDI (chiral ortogonal)	1	1	1	O(N+M) / O(N) × O(M)
CII (chiral symplectic)	-1	1	1	Sp(N+M) /Sp(N) ×Sp(M)
D (BdG)	0	1	0	So(2N)
C (BdG)	0	-1	0	Sp(2N)
DIII (BdG)	-1	1	1	So(2N)/U(N)
CI (BdG)	1	-1	1	Sp(2N)/U(N)

where U is a unitary matrix and K takes the complex conjugate. In the space spanned by eigen-states in Eq. 1.39, U has the form

$$\begin{pmatrix} 0 & -1 \\ 1 & 0 \end{pmatrix}. \tag{1.41}$$

Since the generic Hamiltonian has U(2N) symmetry in order to incorporate the time reversal symmetry in the basis Eq. 1.39 a unitary transformation S must satisfy,

$$\theta = S\theta S^{-1}, \tag{1.42}$$

which defines the Lie group Sp(2N). Therefore the time evolution operator $\exp(itH)$ belongs to the coset space U(2N)/Sp(2N). This method can be used for other symmetries in the table 1.2.

1.3 $\mathbb{Z}_2$ topological insulators

In this section we mainly consider the time reversal $\mathbb{Z}_2$ topological insulators (TRITIs) where, based on the topological classification above belong to the AII class. There

are 2-dimensional and 3-dimensional TIs which are experimentally observed [13]. As we discussed in the previous sections, the topological classification is mainly based on the symmetries that a systems may have. In the time reversal topological insulators the invariance of the Hamiltonian under the action of time reversal operator manifests the concept of topological obstruction:

$$\theta = i\sigma_y K, \tag{1.43}$$

here σ_y is the Pauli matrix and K is taking conjugate. A time reversal Hamiltonian satisfies,

$$\theta H(\vec{k})\theta^{-1} = H(\vec{-k}). \tag{1.44}$$

For spin 1/2 particles the TR operator has the following property

$$\theta^2 = -1. \tag{1.45}$$

This property has an important consequence which is formulated in famous Kramers' theorem : all eigenstates of a TR invariant Hamiltonian are at least two fold degenerate.

Proof: If there exists an eigenstate $|\phi\rangle$ which is not degenerate *i.e.* $T|\psi\rangle = e^{i\phi}|\psi\rangle$ then applying T twice , $Te^{i\phi}|\psi\rangle = |\psi\rangle$ we get a contradiction to the fact that $T^2 = -1$ for spin 1/2 particles.

Some of the properties of a TR operators are :

$$\theta^{-1}\sigma_z\theta = \sigma_z \tag{1.46}$$

$$\theta^{-1}\sigma_x\theta = \sigma_x \tag{1.47}$$

$$\theta^{-1}\sigma_y\theta = \theta^{-1}\begin{pmatrix} 0 & -i \\ i & 0 \end{pmatrix}\theta = \sigma_y \begin{pmatrix} 0 & i \\ -i & 0 \end{pmatrix}\sigma_y = -\sigma_y. \tag{1.48}$$

Since the first Chern number (1.24) was shown in (1.28) to be non zero for systems that break time reversal invariance, first Chern number or TKNN number is zero for time reversal $\mathbb{Z}_2$ topological insulators. However there is an additional topological number that distinguishes the topological states of a $\mathbb{Z}_2$ topological insulator which

is first studied by Kane and Mele. The topological number ν can have two values 0 or 1. The value $\nu = 0$ corresponds to a trivial insulator and the value $\nu = 1$ gives a nontrivial insulator. The concept of existence of a $\mathbb{Z}_2$ number is shown in the schematic figure 1.2 [13]. In the 2-dimensional Brillouin zone there are 4 time reversal invariant points Γ_i, $i = 1, ...4$, which satisfy

$$-\Gamma_i = \Gamma_i + \vec{G}, \tag{1.49}$$

Here $\vec{G}$ is a reciprocal lattice vector. The time reversal invariant Hamiltonian corresponding to an insulator host edge states in the gap between conduction and valance bands. These gap traversing band which are the edge state eigen-energies are degenerate at the four TR invariant points. There are two ways that these bands can traverse the gap they can intersect the Fermi energy E_F either odd number of times or even number of times in half the Brillouin zone, the other half being just the mirror image of it due to TR symmetry.

One of these alternatives is realized depending on the value of the topological number ν. There are several mathematical formulations of the same concept [5,14–16] and we consider only two of these in this thesis.

As we mentioned earlier, the first Chern number is the result of the lack of a smooth global phase to be assigned to the wave function over the magnetic Brillouin zone (which is a torus) due to existence of zeros of the wave function. Therefore the wave function is defined over patches that are related to one another by transition functions and the obstruction comes in to play when one take the integral over the winding number of the transition function over the whole Brillouin zone. This is a consequence of breaking the time reversal in the system, but in $\mathbb{Z}_2$ TI, the first Chern number is zero. However time reversal symmetry imposes a special gauge constraint on the wave function over Brillouin zone which relates the wave functions at $\pm(k, t)$.

$$|u^I_\alpha(-k_1, -k_2)\rangle = \theta|u^{II}_\alpha(k_1, k_2)\rangle \tag{1.50}$$

$$|u^{II}_\alpha(-k_1, -k_2)\rangle = -\theta|u^I_\alpha(k_1, k_2)\rangle. \tag{1.51}$$

Here I and II label the Kramer degeneracy and $\alpha = 1, ..., N$ where N is the number

of bands.

Now lets suppose we define the wave function over four patches.For patch A the wave function $|u^I_\alpha(-k_1,-k_2)\rangle_A$ can be smoothly defined every where in patch A and similarly one can define the wave function smoothly over patch B $|u^I_\alpha(-k_1,-k_2)\rangle_B$. These wave functions are related to each other throughout by the following relation,

$$|u^I_m(-k_1,-k_2)\rangle_A = t^{AB}_{mn}|u^I_n(-k_1,-k_2)\rangle_B. \tag{1.52}$$

The transition matrix is an $m \times n$ matrix which belongs to the unitary group $U(2N)$. Now if we study the change of the $U(1)$ phase of $t_{m,n}$ and take the integral of these changes on the boundary of half of the Brillouin zone then the corresponding winding number is given by:

$$D = \frac{1}{2\pi}\oint_{\partial\tau_1} d\ell[Tr(t^{AB\dagger}\nabla t^{AB})]. \tag{1.53}$$

If D is non zero then there is an obstruction to smoothly defining the wave function on a patch. It can be shown that the above integral can be related to Berry phase and it geometric properties. If now one considers the definition of the Berry vector potential

$$\mathcal{A} = \sum_n i|u_n\langle|\nabla|u_n\rangle_A, \tag{1.54}$$

then the Eq. (1.53)can be written as,

$$D = \frac{1}{2\pi}\oint_{\partial\tau_1} d\ell(\mathcal{A}^B - \mathcal{A}^A). \tag{1.55}$$

This equation can be reformulated by considering the fact that the equation on the boundary $\partial\tau_1$ can be related to regins τ_1 and τ_2. Then using the relation between the closed line integral and surface integral (Stokes theorem),

$$\oint_{\partial\tau_1} d\ell\mathcal{A}^A = \int_{\tau_1} d\tau\mathcal{F}^A, \tag{1.56}$$

one now can rewrite the Eq. (1.55) as,

$$D = \frac{1}{2\pi}[\oint_{\partial\tau_{1/2}} d\ell\mathcal{A} - \int_{\tau_{1/2}} d\tau\mathcal{F}]. \tag{1.57}$$

The patch labels are removed since $\mathcal{F}$ is gauge invariant and the line integral is gauge invariant modulo 2.

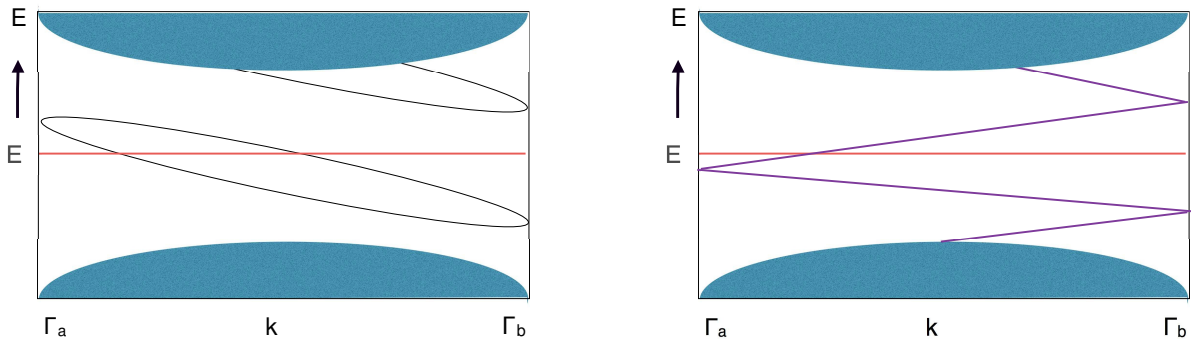

(a) (b)

Figure 1.2: Band structure of a (a) trivial and (b) topological insulator. $\Gamma_a = 0$ and $\Gamma_b = \pi/a$ are two time reversal invariant points. The Kramers partner chafes partner in the topological insulator and they come back together in trivial insulator this also causes the intersection of Fermi energy and the edge states in odd number of time for the topological insulator and even number for the trivial insulator.

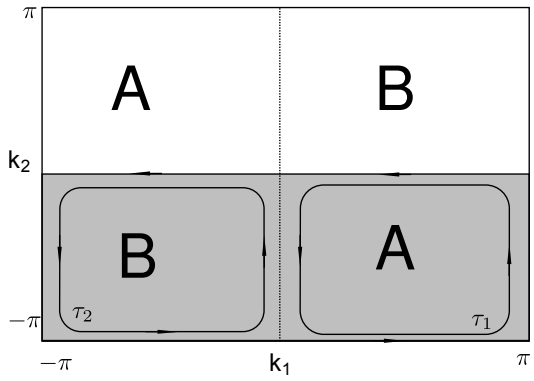

Figure 1.3: The torus defined by k_1 and k_2 divided into two patches A and B. The boundaries of the regions τ_1 and τ_2 are shown as well.

Chapter 2

OPTICAL LATTICES

When an atom is placed in a laser field, the electric field $\vec{E} = \vec{\varepsilon}\widetilde{E}e^{-i\omega t} + (c.c.)$ induces an electric dipole moment $\vec{p}.$ that is proportional to electric field $\overrightarrow{p} = \alpha\vec{E}$ where α is the *complex polarizability* which depends on ω. The interaction potential of the induced dipole moment$\vec{p}$ is given by [17]:

$$U = -\frac{1}{2}\langle\vec{p}.\vec{E}\rangle = -\frac{1}{2\epsilon_0 c}Re(\alpha)I \tag{2.1}$$

where the brackets denote time average. $I = 2\epsilon_0 c|E|^2$ is the intensity of field. The factor $\frac{1}{2}$ has its origin in this fact that $\overrightarrow{p}$ is induced is not intrinsic [18]. Then the force on the atomscan be written as

$$\vec{F}(\vec{r}) = -\nabla U(\vec{r}) = \frac{1}{2\epsilon_0 c}Re(\alpha)\nabla I(\vec{r}). \tag{2.2}$$

The scattering rate Γ_{sc} which can be understood as spontaneous emission of absorbed part of stream of photons with $\hbar\omega$ can be written as , [19]

$$\Gamma_{sc} = \frac{P_{abs}}{\hbar\omega} = \frac{Im(\alpha)I(\vec{r})}{\hbar\epsilon_0 c}. \tag{2.3}$$

In classical models of an atom, electrons are considered to be bound elastically to the core, therfore damping refers to the radiation of oscillating electron. [17]. In order to calculate the polarization one needs to solve the following equation for the x:

$$m[\ddot{\vec{x}} + \gamma\dot{\sigma} + \omega_0\vec{x}] = -e\vec{E}, \tag{2.4}$$

Using of the above equations, the dipole moment can be obtained as

$$\vec{P} = -e\vec{x} = \frac{e^2}{m}(\omega_0^2 - \omega^2 - i\omega\gamma)^{-1}\vec{E}. \tag{2.5}$$

Therefore the polarizability will be given by

$$\alpha = \frac{e^2}{m}\frac{1}{\omega_0^2 - \omega^2 - i\omega\gamma)^{-1}}. \tag{2.6}$$

where

$$\gamma = \frac{e^2\omega^2}{6\pi\varepsilon_0 m_0 c^3}, \tag{2.7}$$

is the classical damping rate due to radiation by dipole. Introducing $\Gamma \equiv (\frac{\omega_0}{\omega})^2\gamma$, we write

$$\alpha = 6\pi\epsilon_0 c^3 \frac{\Gamma/\omega_0^2}{\omega_0^2 - \omega^2 - i(\frac{\omega^3}{\omega_0^2})\Gamma}. \tag{2.8}$$

In a semiclassical approach, the atomic polarizability is calculated as the dipole matrix element between the ground and first excited states

$$\Gamma = \frac{\omega_0^3}{3\pi\epsilon_0\hbar c^3}|\langle e|\mu|g\rangle|^2 \tag{2.9}$$

in case the absolute value of detuning is much larger than Γ, $\Delta = \omega - \omega_0 \gg \Gamma$ the (2.8) becomes

$$V_{dip}(\vec{r}) = -\frac{3\pi c^2}{2\omega_0^3}(\frac{\Gamma}{\omega_0 - \omega} + \frac{\Gamma}{\omega_0 + \omega})I(\vec{r}), \tag{2.10}$$

$$\Gamma_{sc}(\vec{r}) = \frac{3\pi c^2}{2\hbar\omega_0^3}(\frac{\omega}{\omega_0})^3(\frac{\Gamma}{\omega_0 - \omega} + \frac{\Gamma}{\omega_0 + \omega})^2 I(\vec{r}). \tag{2.11}$$

Usually the laser is tuned relatively close to resonance at ω_0, that is $|\Delta| = |\omega - \omega_0| \ll \omega_0$, so that rotating-wave approximation can be used. This means neglecting high frequencies. Therefore the following result will be obtained,

$$V_{dip}(\vec{r}) = \frac{3\pi c^2}{2\omega_0^3}\frac{\Gamma}{\Delta}I(\vec{r}), \tag{2.12}$$

$$\Gamma_{sc}(\vec{r}) = \frac{3\pi c^2}{2\hbar\omega_0^3}(\frac{\Gamma}{\Delta})^2 I(\vec{r}). \tag{2.13}$$

From here we can deduce a simple relation between V_{dip} and Γ_{sc};

$$\hbar\Gamma_{sc} = \frac{\Gamma}{\Delta}V_{dip} \tag{2.14}$$

which describe the main characteristic of a dipole potential. For $\Delta < 0$, $V_{dip} < 0$ the dipole provides an attractive potential and its minimum is the position of maximum intensity (red-tuned). For the case $\Delta > 0$,$v_{dip} > 0$ on the other hand, the potential is repulsive and pushes the atoms out of the high intensity region (blue-tuned).

2.1 Atomic Hamiltonian

The Hamiltonian for an atom which interacts with an electro magnetic field can be written as [18]

$$H = \frac{1}{2m}[\vec{p} - e\vec{A}(\vec{r},t)]^2 + eV(\vec{r}) \tag{2.15}$$

where $\vec{p}$ is the momentum of the electron, $V(r)$ is the Coulomb potential, $\vec{A}$ is the vector potential. If we use the following unitary transformation

$$|\Psi(t)\rangle = exp[\frac{ie\vec{r}.\vec{A}(\overrightarrow{r},t)}{\hbar}]|\chi(t)\rangle \equiv U|\chi(t)\rangle \tag{2.16}$$

and substitute into the Shrödinger equation we will get the Shrödinger equation as follows

$$i\hbar\frac{\partial|\Psi(t)\rangle}{\partial t} = H|\Psi(t)\rangle, \tag{2.17}$$

$$i\hbar U\frac{\partial|\chi(t)\rangle}{\partial t} + i\hbar\frac{\partial U}{\partial t}|\chi(t)\rangle = HU|\chi(t)\rangle. \tag{2.18}$$

Multiplying them by $U^\dagger$ leads to

$$i\hbar\frac{\partial|\chi(t)\rangle}{\partial t} = H'|\chi(t)\rangle, \tag{2.19}$$

$$H' \equiv U^\dagger HU - i\hbar U^\dagger\frac{\partial U}{\partial t}. \tag{2.20}$$

The second term above gives the dipole interaction

$$-i\hbar U^\dagger\frac{\partial U}{\partial t} = e\vec{r}.\frac{\partial\vec{A}}{\partial t} = -e\vec{r}.\vec{E}(\vec{r},t). \tag{2.21}$$

By working out $U^\dagger HU$ and fixing the gauge $\nabla.\vec{A} = 0$ one gets,

$$U^\dagger HU = eV(r)\frac{\vec{p}^2}{2m} + \frac{e}{m}\sum x_i\frac{\partial A_i}{\partial x_j}p_j,$$

$$\frac{e\hbar}{2mi}\sum_{ij} x_i\frac{\partial^2 A_i}{\partial x_j^2} + \frac{e^2}{2m}\sum_{ijk}\frac{\partial A_i}{\partial x_k}\frac{\partial A_j}{\partial x_k}. \tag{2.22}$$

Then making use of the standard dipole approximation,

$$\vec{A}(\vec{r}) = \vec{A}_0 e^{-i\omega t + i\vec{k}.\vec{r}} \to A_0 e^{-i\omega t + i\vec{k}.\vec{r}_0} = \vec{A}(\vec{r}_0), \tag{2.23}$$

where $\vec{r_0}$ is the position of the atomic nucleus, i.e. assuming that the radiation wave length is much larger than the atomic size, we obtain finally

$$H' = \hbar \sum_i \omega_i |i\rangle\langle i| - e\vec{r}.\vec{E}(\vec{r}, t). \tag{2.24}$$

2.2 Two-level atom interacting with a single field mode

As it is discussed in the last section, an atom interacts with a photon through the dipole interaction

$$H = -e\vec{r}.\vec{E} \tag{2.25}$$

where using quantized version of the electrical field we have

$$E(z) = \epsilon(a + a^\dagger) \sin kz. \tag{2.26}$$

$\epsilon = \sqrt{\frac{\hbar\omega}{\epsilon_0 v}}$ is the field amplitude per photon, and the interaction Hamiltonian can be written. The dipole is induced by the electric field alone and we assumed that dipole has just non-diagonal matrix element.

$$H_I = \hbar g(\sigma_+ + \sigma_-)(a + a^\dagger), \tag{2.27}$$

where $g \equiv -(\frac{\epsilon d}{\hbar}) \sin kz$,$d = e\vec{r}_{ab}.\vec{e}$ and σ are the usual Pauli matrices

$$\sigma_+ = \begin{pmatrix} 0 & 1 \\ 0 & 0 \end{pmatrix} \; \sigma_- = \begin{pmatrix} 0 & 0 \\ 1 & 0 \end{pmatrix}. \tag{2.28}$$

The complete Hamiltonian can be written now as:

$$H_1 = \frac{\hbar\omega_{ab}}{2}\sigma_z + \hbar g(\sigma_+ + \sigma_-)(a + a^\dagger). \tag{2.29}$$

Here the zero energy has been taken to lie halfway between the two atomic energy levels. The interpretation of various terms in the above formula is as follows :

$a\sigma_+$: excitation of one atom by absorbing one photon,

$a^\dagger\sigma_+$: emission of one photon and de-excitation of atom,

$a^\dagger\sigma_+$: emission one photon and the atom excitation of

$a\sigma_-$ absorption of one photon and de-excitation of atom. In the interaction picture we write

$$H_1^I = \hbar g(\sigma_+ a e^{-i(\omega-\omega_{ab})t} + \sigma_- a^\dagger e^{i(\omega-\omega_{ab})t} + \sigma_- a e^{-i(\omega+\omega_{ab})t} + a^\dagger \sigma_+ e^{i(\omega+\omega_{ab})t}), \quad (2.30)$$

we may neglect terms with $\omega + \omega_{ab}$ since theyare oscillating very fast . Thus we reach the Jaynes-Cummings Hamiltonian we have

$$H = \frac{\hbar\omega_{ab}}{2}\sigma_z + \hbar\omega a^\dagger a + \hbar g(a\sigma_+ + \sigma_- a^\dagger). \quad (2.31)$$

It can be shown that in an appropriate basis, the atom-photon coupling in rotating wave approximation using similar steps can be written as

$$H = \begin{pmatrix} \hbar\omega + \frac{\hbar\omega_{ab}}{2} & \hbar g \\ \hbar g & \hbar\omega - \frac{\hbar\omega_{ab}}{2} \end{pmatrix}. \quad (2.32)$$

In the next chapter, we will use similar couplings that corresponds to spin-orbit coupling to create an artificial gauge for an atom.

Chapter 3

$\mathbb{Z}_2$ TOPOLOGICAL INSULATOR ON OPTICAL LATTICES

3.1 Introduction

As we mentioned in the introduction 1, it is widely acknowledged that the cold atomic systems are ideal systems to simulate solid-state phenomena in a controlled way. The two and three dimensional topological insulators with band gaps in the order of the recoil energy have recently been proposed in ultracold fermionic atomic gases [6]. The proposal utilizes interactions which preserves time reversal symmetry (TRS), analogous to synthesized spin-orbit coupling [20], so that the insulators are classified by the so called $\mathbb{Z}_2$ topological invariant [21].

Even if the band gap in tight binding models are not as large as in nearly free electron limit, TIs in ultra cold atomic systems have been studied vastly in tight binding regime [22, 23]. The optical lattices are described by continuous potentials formed by the combinations of standing waves. It is convenient to treat them as deep potentials. Our aim in this article is to study the tight binding limit of the quantum spin Hall effect which can be realized in the ultracold atomic systems. The corresponding model in the nearly free electron limit is proposed in [6] with this advantage that the band gap is large.

3.2 Model system

In this section we review briefly the $\mathbb{Z}_2$ topological insulator model proposed by Béri and cooper [6]. The Hamiltonian of an atom with N internal states with position $\mathbf{r}$

and momentum $\mathbf{p}$ can be written as,

$$H = \frac{\mathbf{p}^2}{2m} + \hat{V}(\mathbf{r}), \tag{3.1}$$

here $\hat{V}(\mathbf{r})$ is a position dependent potential which is a $N \times N$ matrix acting on the internal states of the atom. A $\mathbb{Z}_2$ topological insulator is invariant under the action of time-reversal operator $\Theta = i\sigma_y\hat{K}$, where $\sigma_{x,y,z}$ are Pauli matrices acting on electronic spin and $\hat{K}$ is complex conjugation operator. The general form of the a time reversal invariant potential in the form of a matrix can be written as,

$$\hat{V}(\mathbf{r}) = \begin{pmatrix} (A+B)\mathbb{1}_2 & C\mathbb{1}_2 - i\sigma\cdot\mathbf{D} \\ C\mathbb{1}_2 + i\sigma\cdot\mathbf{D} & (A-B)\mathbb{1}_2 \end{pmatrix}. \tag{3.2}$$

Here A,B and C are real numbers, $\mathbf{D}$ is a 3-vector with real components and $\mathbb{1}_2$ is 2×2 identity matrix. $N = 4$ for the smallest potential which can be used to create a $\mathbb{Z}_2$ topological insulator.

This Hamiltonian can be realized using an atom with four internal states as proposed by [6]. Ytterbium ^{171}Yb, which has nuclear spin $I = 2$, is a good candidate for this purpose. It has a $2-$fold degenerate ground state ($^1S_0 = g$) and a long-lived $2-$fold degenerate excited state ($^3P_0 = e$). Another advantage of Yb is the existence of a state dependent scalar potential for a specific wavelength λ_{magic} [1] in which the potential changes sign and becomes $\pm V_{\text{am}}(\vec{r})$ for the ground and excited states.

All the $e-g$ transitions, shown in Fig. 3.1, have the same frequency $\omega_0 = (E_e - E_g)/\hbar$. The electric field of the lasers interacting with the atom is $\vec{E} = \vec{\epsilon}e^{-i\omega t} + \vec{\epsilon}^* e^{i\omega t}$. The potential in the rotating wave approximation then can be expressed as [18], This model is studied in nearly free electron limit which has the advantage of large band gap.

Using rotating wave approximation [18] we have the optical potential as following,

$$V\hat{M}(\vec{r}) = \begin{pmatrix} (\frac{\hbar}{2}\Delta + V_{\text{am}})1 & -i\vec{\sigma}.\vec{\varepsilon}d_r \\ i\vec{\sigma}.\vec{\varepsilon}d_r & -(\frac{\hbar}{2}\Delta + V_{\text{am}}) \end{pmatrix} \tag{3.3}$$

where $\Delta = \omega - \omega_0$ is the atom-field detuning and d_r is the dipole moment. One can

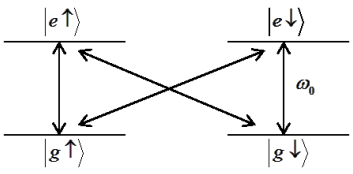

Figure 3.1: The atomic levels of Ytterbium and the interactions between atoms and lasers

write the hamiltonian in terms of Dirac matrices [24],

$$\Gamma^{1,2,3} = -i\sigma^y \otimes \sigma^i, \Gamma^4 = \sigma^x \otimes I \text{ and } \Gamma^5 = \sigma^z \otimes I, \tag{3.4}$$

which gives,

$$H = \frac{\hat{\mathbf{P}}^2}{2m}\mathbb{1} + \Gamma^i d_r \varepsilon_i + \Gamma^5(\frac{\hbar}{2}\Delta + V_{\text{am}}). \tag{3.5}$$

For the two-dimensional system one can make following choice for the potential matrix Eq. (3.3):

$$\begin{aligned} d_r\epsilon &= [V\delta, V\cos(\vec{r}.\vec{k}_1), V\cos(\vec{r}.\vec{k}_2)], \\ \frac{\hbar}{2}\Delta + V_{am}(\vec{r}) &= V\cos(\vec{r}.(\vec{k}_1 + \vec{k}_2)) \end{aligned} \tag{3.6}$$

with $\vec{k}_1 = k(1,0,0)$ and $\vec{k}_2 = k(\cos(\theta), \sin(\theta), 0)$.

The optical potential in Eq. (3.3) is formed from three standing waves which are linear polarized light at the coupling frequency ω. Two of these waves have equal amplitude in the 2D plane ($\vec{k}_1$ for y polarization and $\vec{k}_2$ for $\vec{z}$ polarization) the $\vec{x}$ polarized wave vector is normal to the 2D plane with an amplitude smaller by a factor of δ. Since the $\omega \simeq \omega_0$, we have $k \simeq 2\pi/\lambda_0$ with $\lambda_0 = 578$ nm the wavelength of the e-g transition. The spatial dependence of V_{am} is set by a standing wave at the antimagic wavelength λ_{am} [1], which creates a state-dependent potential with $|\vec{k}_1 + \vec{k}_2| = 4\pi/\lambda_{\text{am}}$ that leads $\theta = 2\arccos(\pm\lambda_0/\lambda_{\text{am}})$. For simplicity, in all following discussions one can fix $\theta = 2\pi/3$ and define $a \equiv 4\pi/(\sqrt{3}k)$. Therefore the optical coupling $\hat{M}$ has the symmetry of a triangular lattice. In Fig. 3.2a we show the few lowest energy bands for $\delta = 0$. The bands were calculated by numerical diagonalization in the plane wave

basis (49 plane waves is used). All bands are fourfold degenerate similar to tight binding regime.

We also calculated the density of states (DOS) for the Hamiltonian in Eq. (3.5). This quantity is defined by the expression,

$$\rho(E) = \frac{1}{S}\sum_{\mathbf{k}} \delta(E - E_n), \tag{3.7}$$

where S is the area of the system in reciprocal space and E_n is the energy of the bands. The DOS for the nearly free electron limit is depicted in Fig. 4.2c.

To pave the way toward the tight binding limit we consider the deep potential limit $V \gg \hbar k^2/2M$ [25] that is when the potential part of the Hamiltonian Eq. (3.1) plays the dominant role. As unitary transformation preserves the physical aspect of the system in order to find the lattice points of the system in a simple form we apply the unitary transformation $\hat{U} = (\mathbb{1} - i\hat{\Sigma}_3\hat{\sigma}_2)/\sqrt{2}$ to the coupling $\hat{M}$ in Eq. (3.3):

$$\hat{M}' = \hat{U}^\dagger \hat{M} \hat{U} = c_1\hat{\Sigma}_1 + c_2\hat{\Sigma}_2\sigma_3 + c_{12}\hat{\Sigma}_3. \tag{3.8}$$

here $\Sigma_i = \sigma_i \otimes \mathbb{1}_{2\times 2}$, $c_i \equiv \cos(\mathbf{r}\cdot\mathbf{k_i})$ and $c_{12} = \cos(\mathbf{r}\cdot(\mathbf{k}_1 + \mathbf{k}_2))$. In order to find the minima of the adiabatic energy which gives the lattice sites in tight binding regime [26]. We diagonalized the potential in Eq. (3.8) analytically and obtained,

$$V_{\text{ad}} = \pm\sqrt{c_1^2 + c_2^2 + c_{12}^2}, \tag{3.9}$$

as plotted in Fig. 3.3.

3.3 Calculation of band structure

In order to calculate band structure we used the plane wave method in which we write the wavefunction as [27]

$$\psi_{\vec{k}}(\vec{r}) = u_{\vec{k}} e^{i(\vec{k}.r)} \tag{3.10}$$

where $u_{\vec{k}}(\vec{r})$ has the period of the lattice with $u_{\vec{k}}(\vec{r}) = u_{\vec{k}}(\vec{r}+\vec{T})$. Here $\vec{T}$ is a translation vector of the lattice.

since our potential is invariant under lattice translation, we may expand it as Fourier series in the reciprocal lattice vector $\vec{G}$.

$$U(\vec{r}) = \sum_{\vec{G}} U_{\vec{G}} e^{i\vec{G}.\vec{r}} \tag{3.11}$$

where

$$U_{\vec{G}} = \frac{1}{area} \int_{unitcell} U(\vec{r}) e^{-i\vec{G}.\vec{r}} d^3r$$

The wave equation is $H\psi = E\psi$, where H is the Hamiltonian and E is the energy eigenvalue. Its explicit form reads as following

$$(\frac{1}{2m}p^2 + U(\vec{r}))\psi(\vec{r}) = e\psi(\vec{r}) \tag{3.12}$$

we may write the wavefunction as a Fourier series summed over all the values of the wave vector,

$$\psi = \sum_{\vec{k}} C(\vec{k}) e^{i\vec{k}.\vec{r}}, \tag{3.13}$$

the values of $\vec{k}$ can be $\frac{2\pi n}{L}$,because these values satisfy periodic boundary conditions over length L.

In order to solve the wave equation, we substitute (3.12) in (3.13), which leads to a set of linear algebraic equations for the Fourier coefficients. The kinetic energy term is

$$\frac{1}{2m}\vec{p}^2\psi(\vec{r}) = \frac{\hbar^2}{2m} \sum_{\vec{k}} |\vec{k}|^2 C(\vec{k}) e^{i\vec{k}.\vec{r}} \tag{3.14}$$

and the potential term is

$$(\sum_{\vec{G}} U_{\vec{G}} e^{i\vec{G}.\vec{r}})\psi(\vec{r}) = \sum_{\vec{G}} \sum_{\vec{k}} U_{\vec{G}} C(\vec{k}) e^{i(\vec{k}+\vec{G}).\vec{r}} \tag{3.15}$$

submitting 3.15in 3.14 we get

$$\sum_{\vec{k}} \frac{\hbar^2}{2m} |\vec{k}|^2 C(\vec{k}) e^{i\vec{k}.\vec{r}} + \sum_{\vec{G}} \sum_{\vec{k}} U_{\vec{G}} C(\vec{k}) e^{i(\vec{k}+\vec{G}).\vec{r}} = E \sum_{\vec{k}} C(\vec{k}) e^{i\vec{k}.\vec{r}} \tag{3.16}$$

This equation can be satisfied if each Fourier component has the same coefficient on both sides of the equation. Therefore we have the centeral equation:

$$(\frac{\hbar^2}{2m} - E)C(\vec{k}) + \sum_{\vec{G}} C(\vec{k} - \vec{G}) = 0 \tag{3.17}$$

This equation has infinite number of $C(\vec{k}-\vec{G})$ to be determined but in practice small number of them suffice.

3.4 Tight binding model for $\mathbb{Z}_2$ topological insulator on a triangular lattice

In the deep lattice limit $V \gg \hbar^2 k^2/2M$ we can use the Wannier functions as suggested in Ref. [28]. There are four Wannier functions $\omega_{\alpha,\sigma}(\mathbf{r})$ where $\alpha \in e, g$ and $\sigma \in \uparrow, \downarrow$. We express the Hamiltonian in terms of these Wannier functions.

$$\begin{aligned} H &= \sum_{<mn>} t_1 D^\dagger_{m+1,n} s_z D_{m,n} - i t_2 D^\dagger_{m+1,n+1}(\delta\sigma_x + \\ &\quad \sigma_y + \sigma_z) D_{m,n} + t_2 D^\dagger_{m,n+1}\left(\delta\sigma_x + \sigma_y + \sigma_z\right) D_{m,n} \\ &\quad + \epsilon D^\dagger_{m,n} D_{m,n} + H.c., \end{aligned} \tag{3.18}$$

Here $D_{m,n}$ and $D^\dagger_{m,n}$ are annihilation and creation operators respectively and the spin index is suppressed. The hopping parameters are given by

$$\begin{aligned} t_1 &= \int \omega_{A,\alpha}(r_{m+1,n+1}) V \cos((\mathbf{k}_1 + \mathbf{k}_2)\cdot\mathbf{r}) \omega_{B,\beta}(r_{m,n}) d^2\mathbf{r} \\ &= \int \omega_{A,\alpha}(r_{m,n+1}) V \cos((\mathbf{k}_1 + \mathbf{k}_2)\cdot\mathbf{r}) \omega_{B,\beta}(r_{m,n}) d^2\mathbf{r} \end{aligned} \tag{3.19}$$

$$\begin{aligned} t_2 &= \int \omega_{A,\alpha}(r_{m+1,n}) V \cos(\mathbf{k}_i \cdot \mathbf{r}) \omega_{B,\beta}(r_{m,n}) d^2\mathbf{r} \\ &\quad \text{for i=1,2,} \end{aligned} \tag{3.20}$$

$$\text{and the on site energy } \epsilon = \int \omega_{\alpha,\sigma}(r_{m,n}) \omega_{\alpha,\sigma}(r_{m,n}) d^2\mathbf{r}. \tag{3.21}$$

The Wannier functions are the solutions of the Hamiltonian in Eq. (3.1) without the off-diagonal elements in Eq. (3.3) which tend towards Gaussian state wave function localized in lattice sites $\mathbf{r}_{m,n}$ [1]. Accordingly the hopping coefficients and on-site energy

are independent of spin and site index. The Fourier transform of above Hamiltonian in momentum space is:

$$\begin{bmatrix} A+\epsilon & 0 & -iB & (-i\delta-1)B \\ 0 & A+\epsilon & (-i\delta+1)B & iB \\ iB & (i\delta+1)B & -A+\epsilon & 0 \\ (i\delta-1)B & -iB & 0 & -A+\epsilon \end{bmatrix}, \tag{3.22}$$

here $A = d_{12}$, $B = d_1 + d_2$ where d_{12}, d_1 and d_2 are defined to be,

$$d_1 = t_2 \cos\left(k_y a/2\right), \tag{3.23}$$

$$d_2 = t_2 \cos\frac{a}{4}\left(\sqrt{3}k_x + k_y\right), \tag{3.24}$$

$$d_{12} = t_1 \cos\frac{a}{4}\left(\sqrt{3}k_x - k_y\right). \tag{3.25}$$

The band structure of Eq. (3.22) is shown in Fig. 3.4a We take $\delta = 0$ as its small values do not affect the band structure while its large values ($\delta \gg 1$) closes the gap both in the nearly free electron and in the tight binding limits.

The difference is in the $(0, 0)$ point in k-space where the upper band of cold atom limit has a sharper peak Fig. 3.2a than the tight binding upper band Fig 3.4a. This can be understood as the characteristic behavior of the energy levels of free electron which are just a parabola in k (momentum), by getting distorted due to a periodic potential [29]. As the potential becomes stronger the energy dispersion resembles the tight binding regime Fig. 3.4a. The comparison of the DOS of the nearly free electron limit as is depicted in Fig. 3.2c shows that states are distributed around the two energy bands across the gap asymmetrically due to the asymmetrically located van Hove singularities of the upper and lower bands in contrast to that of tight binding case in Fig. 3.4b. Since in the Fig. 3.4a we have the $\epsilon = 0$ the system has particle hole symmetry which with time reversal symmetry, the topological class of the system will be different but as $\epsilon \neq 0$ in the tight binding limit the system will be in class AII which is the class of quantum spin Hall [12]. Summarizing, we developed a tight binding model of the $\mathbb{Z}_2$ topological insulator system of ultra cold atoms in a triangular optical lattice that is proposed and examined in Ref. [6] in the nearly free electron limit. We

find the band structure and density of states in the tight binding and in the nearly free electron cases and compare them. Quantum spin Hall symmetry class of AII is verified for the tight binding model

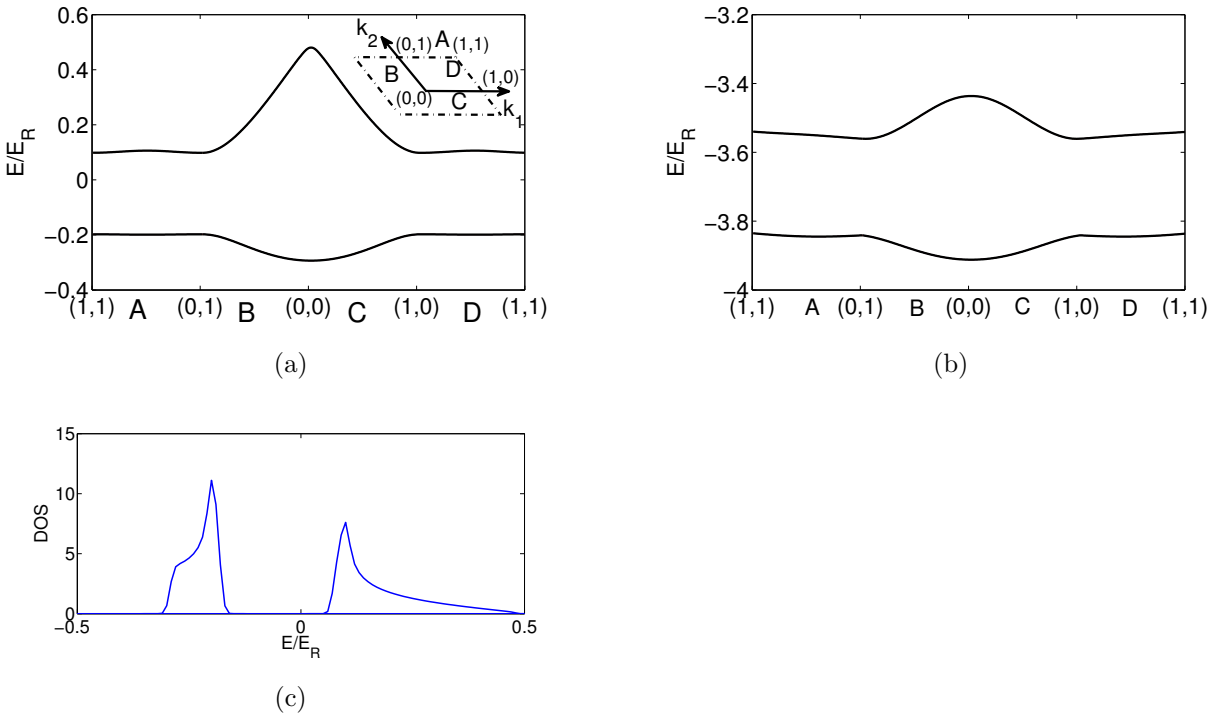

Figure 3.2: (a) Lowest energy bands of the cold atom system in nearly free electron limit as the result of the solution of Eq. (3.5). The energy is plotted relative to recoil energy E_R. Here $V = 0.5E_R$ and $\delta = 0$ are shown here. The k-points are labeled as $\vec{\Gamma}_{mn} = (m\vec{k}_1 + n\vec{k}_2)/2$ and each band is four fold degenerate.(b) Energy bands for the potential $V = 3.5E_R$ which resembles the band structure of tight binding regime of Eq. 3.1. (c) DOS of the energy bands in Fig. 3.2a which are depicted in the band structure is shown. Energy is expressed in the unit of E_R

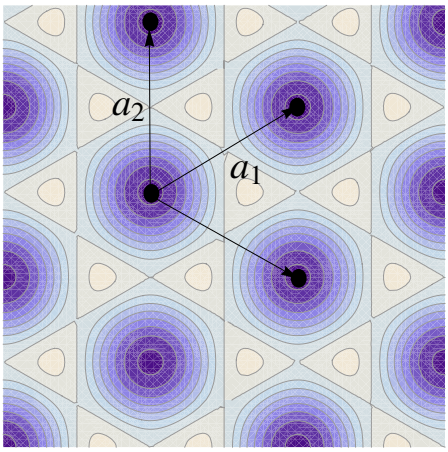

Figure 3.3: The dark circles show the local minima of the adiabatic energy Eq. (3.9) which forms a triangular lattice in the tight binding limit. Energy and length are dimensionless and scaled by V and a, respectively.

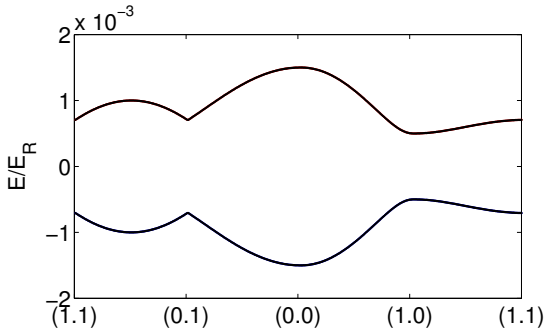

(a)

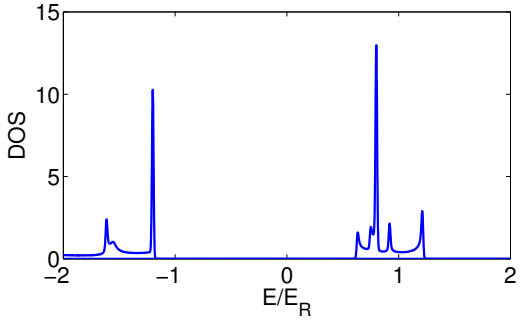

(b)

Figure 3.4: The band structure of the Hamiltonian Eq. (3.22) along the path (1,1), (1,0), (0,0), (0,1) where 1 and 0 are referring to the inset (m,n) in $\vec{\Gamma}_{mn} = (m\vec{k}_1 + n\vec{k}_2)$, which are the TRS invariant points in Brillouin zone. We took $\epsilon = 0$, V $= 15E_R$, $\delta = 0$ and $t_1 = t_2 = t \approx 10^{-3}$ [1] . (b) DOS of the energy bands which are depicted.

Chapter 4

$\mathbb{Z}_2$ TOPOLOGICAL INSULATOR ON TRIANGULAR BICHROMATIC OPTICAL LATTICES

4.1 Introduction

Topological insulators are insulating in the bulk but have metallic states on their boundaries [13, 15]. Robustness of these states against disorder and perturbations makes them promising for applications such as spintronics [14] and topological quantum computation [30]. Topological invariants of the bulk material are essential for the robust boundary modes. This urged consideration of topological insulators on different lattice geometries [31–35]. Testing these systems against strong disorder and perturbations is challenging both experimentally and theoretically. Detailed numerical investigations reveal that topological protection is safe only for surface disorder smaller than the bulk band gap [36].

Two and three dimensional topological insulators with band gaps in the order of the recoil energy have recently been proposed in ultracold fermionic atomic gases [6]. This large gap systems are described in the nearly free electron limit, which is a different perspective to examine topological insulators compared to earlier studies [22, 23]. The proposal utilizes interactions which preserves time reversal symmetry (TRS), analogous to synthesized spin-orbit coupling [20], so that the insulators are classified by the so called $\mathbb{Z}_2$ topological invariant [35].

Our aim in this article is to examine robustness of two dimensional $\mathbb{Z}_2$ topological insulators [6] against large global perturbations that preserves TRS. Motivated by their recent use in quantum simulations of relativistic field theories [37, 38] and disorder induced localization [39–41], we specifically consider here bichromatic optical

lattice perturbations. Similar studies of $\mathbb{Z}_2$ topological insulators in bichromatic potentials, but for a one-dimensional optical lattice in tight-binding limit, reveals that topological properties of the system can be probed by density measurements [42, 43].

This report is organized as follows. In Sec. 5.3 we briefly review the proposal of $\mathbb{Z}_2$ topological insulator in ultracold atomic gases [6], and introduce the bichromatic deformation of the lattice potential terms. In Sec. 4.3 we describe the method of calculation of the $\mathbb{Z}_2$ invariant in the case of absence of inversion symmetry [5] and present the corresponding results.

4.2 Model system

We start with Eq. (3.3) from previous chapter. Rewriting it in following form will be convenient to show the modification to incorporate the bichromatic lattice,

$$\hat{V} = \begin{pmatrix} (\frac{\hbar}{2}\Delta + V_{\text{am}})\mathbb{1}_2 & -i\sigma.\epsilon d_r \\ i\sigma.\epsilon d_r & -(\frac{\hbar}{2}\Delta + V_{\text{am}})\mathbb{1}_2 \end{pmatrix}, \tag{4.1}$$

where $\Delta = \omega - \omega_0$ and d_r is the reduced dipole moment of the atom [44].

The two-dimensional triangular lattice is given by the following elements of the potential matrix,

$$d_r\epsilon = [V\delta, V\cos(\vec{r}.\vec{k}_1), V\cos(\vec{r}.\vec{k}_2)], \tag{4.2}$$

$$\frac{\hbar}{2}\Delta + V_{\text{am}}(\vec{r}) = V\cos(\vec{r}.(\vec{k}_1 + \vec{k}_2)) \tag{4.3}$$

with $\vec{k}_1 = k(1, 0, 0)$ and $\vec{k}_2 = k(\cos(\theta), \sin(\theta), 0)$. Since $\omega \simeq \omega_0$, we have $k \simeq 2\pi/\lambda_0$ with $\lambda_0 = 578$ nm the wavelength of the $e - g$ transition. The spatial dependence of V_{am} is set by a standing wave at the antimagic wavelength λ_{am} which creates a state-dependent potential with $|\vec{k}_1 + \vec{k}_2| = 4\pi/\lambda_{\text{am}}$ that leads to $\theta = 2\arccos(2\pi/3)$. We define $a \equiv 4\pi/(\sqrt{3}k)$. Therefore the optical potential has the symmetry of a triangular lattice with lattice vectors $\vec{a}_1 = (\sqrt{3}/2, -1/2)a$ and $\vec{a}_2 = (0, 1)a$. The Hamiltonian Eq. (3.1) with potential part Eq. (4.1) is invariant under translation by the lattice vectors $\vec{a}_i$. Therefore using the associated reciprocal vectors we can define

the Bloch Hamiltonian,

$$\hat{H}_{\vec{k}} = \frac{(\hat{p} + \hbar\vec{k})^2}{2m}\mathbb{1}_N + \hat{V}'(\vec{r}), \tag{4.4}$$

here $\vec{k}$ is the conserved momentum. $\hat{V}' = U^{-1}\hat{V}U$ where $U = 2^{-1/2}(\mathbb{1}_4 - i\Sigma_3\sigma_2)$ is a unitary transformation. The potential $\hat{V}'$ takes the following form:

$$\hat{V}' = c_1\Sigma_1 + c_2\Sigma_2\sigma_3 + c_{12}\Sigma_3 + \delta\Sigma_2\sigma_1. \tag{4.5}$$

Here $c_{1(2)} = \cos(\mathbf{r}\cdot\mathbf{k}_{1(2)})$ and $c_{12} = \cos(\mathbf{r}\cdot(\mathbf{k}_1 + \mathbf{k}_2))$

In the absence of the bichromatic lattice the Hamiltonian Eq. (4.4) is invariant under the half translational symmetries $T_1 = \Sigma_2 T_{\vec{a_1}/2}$ and $T_2 = \Sigma_1\sigma_3 T_{\vec{a_2}/2}$ where $T_{\vec{a_i}}$ is translation operator along the lattice vector $\vec{a_i}$.

In order to examine the robustness of the $\mathbb{Z}_2$ topological insulator to strong perturbations we introduce bichromatic deformations. For simplicity, we do not change the angular orientation of the lattice so that the angular variable θ is not affected by the deformation. This can be accomplished by not deforming the element introduced in Eq. (4.3). In addition, we do not deform the first component in the element Eq. (4.2). The δ dependent component plays the role of the spin orbit coupling to hybridize the lower bands of the two optical flux lattices. We choose not to perturb this essential process that mixes these bands with the non-trivial Chern numbers.

The bichromatic deformation is introduced in the remaining two terms such that

$$\begin{aligned} d_r\vec{\epsilon} &= [V\delta, V\cos(\vec{r}.\vec{k}_1) + V'\cos(2\vec{r}.\vec{k}_1 + \phi), \\ &\quad V\cos(\vec{r}.\vec{k}_2) + V'\cos(2\vec{r}.\vec{k}_2 + \phi)], \\ \frac{\hbar}{2}\Delta + V_{\mathrm{am}}(\vec{r}) &= V\cos(\vec{r}.(\vec{k}_1 + \vec{k}_2)) \\ &\quad + V''\cos(2\vec{r}.(\vec{k}_1 + \vec{k}_2) + \phi'). \end{aligned}$$

Here we examine the case where $\phi = \phi' = 0$. This model is unitarily equivalent to the superposition of two bichromatic optical flux lattices that is coupled with a spin-orbit type interaction [6]. Such a configuration is illustrated in the Fig. 4.1b which is the cross section view of the potential along the $\vec{k}_1$ direction. We explore its effect on the topological character of the insulator in the next section.

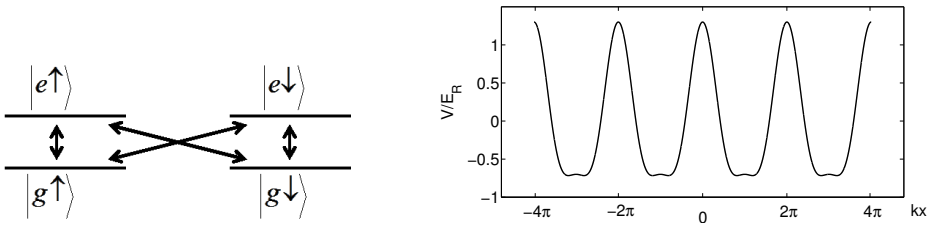

(a) (b)

Figure 4.1: (a) Optical transitions between the ground (g) and excited (e) energy levels. Two-fold nuclear spin degeneracy yields the manifold of states $|g\uparrow\rangle$, $|g\downarrow\rangle$, $|e\uparrow\rangle$ and $|e\downarrow\rangle$ used to define the potential matrix in Eq. (4.1) (b) The schematic view of the cross section of the bichromatic optical lattice along the $\vec{k}_1$ direction, for the case $V' = 0.2V$.(All quantities plotted are dimensionless)

4.3 Results

We determine the topological character of the insulator directly using the band structure to calculate the $\mathbb{Z}_2$ invariant. The Hamiltonian in Eq. (**??**) can be numerically diagonalized using plane-wave method. The band structure is shown in Fig. 4.2. The Lowest twofold degenerate energy bands for the lattice without disorder Fig. 4.2a has no gap between first and second bands. As we introduce the bichromatic lattice along different direction the fourfold degeneracies at special points in k-space are lifted. For the cases when the potential strength are as large as $V' = 0.5V$ and $V'' = 0.5V$ Fig. 4.2b shows a gap opening between first and second bands but it is very narrow. Fig. 4.2c shows a gap opening for the case $V' = 0.5V$and $V'' = 0.5V$.

In order to investigate the topological state of the system we use the method in Ref. [5]. There are other methods to determine the topological characteristic of the systems where the detailed discussion and the relevant mathematical methods and the advantages and shortcoming of different approaches on the calculation of $\mathbb{Z}_2$ invariant can be found in the literature [**?**, **?**, 5, 15, 16, 45]. In the case of inversion symmetric materials, finding the $\mathbb{Z}_2$ can be done using the Fu and Kane method [21].

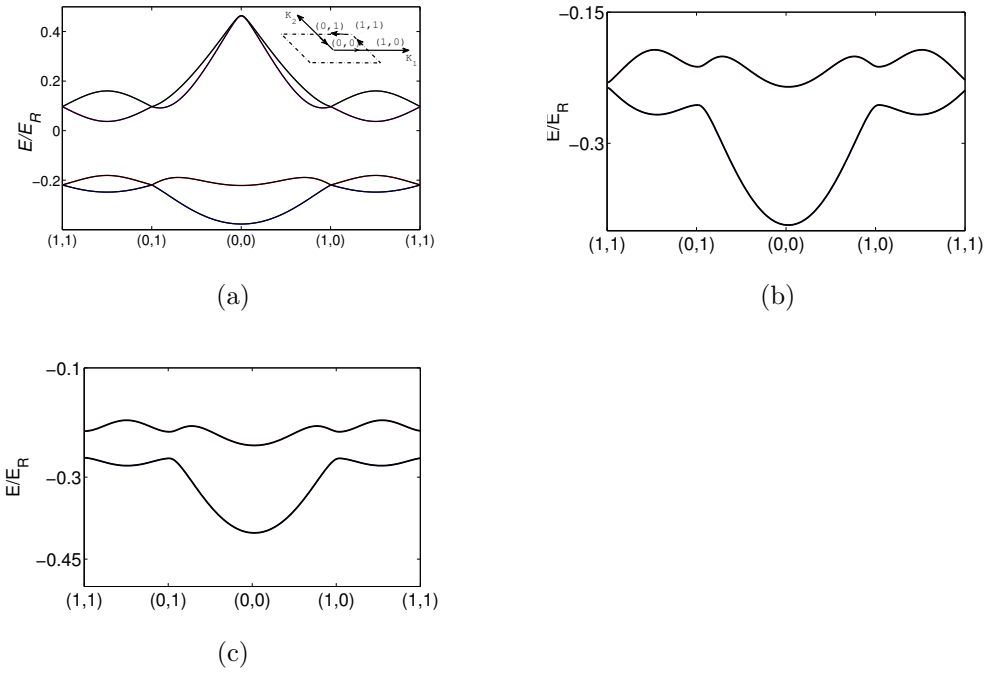

Figure 4.2: Lowest energy bands for the lattice with $V = 0.5E_R$ are shown for the cases of (a) $V' = V'' = 0$ and (b) $V' = 0.5V$ and $V'' = 0$ (c) $V' = 0.5V$and $V'' = 0.5V$. The $\vec{k}$-points are labeled as ($\vec{\Gamma}_{pq} = (p\vec{k}_1 + q\vec{k}_2)/2$) and indicated in the figure by (p, q) with $p, q \in \{0, 1\}$, here $\mathbf{k}_1$ and $\mathbf{k}_2$ are reciprocal lattice vectors. At the special points (1,0), (1,1) and (0,1) the fourfold degeneracy is reduced to twofold by the presence of bichromatic lattice potential.

Since the parity and time-reversal operators commute, we only need to check the parity eigenvalues in four time-reversal invariant points in k-space for all bands below the gap. The result for the system, without bichromatic deformation, turns out to be non-trivial so that it is either a $\mathbb{Z}_2$ insulator or a quantum spin Hall insulator, depending on the presence or absence of δ coupling, respectively [6].

4.3.1 Pfaffian

The Hilbert space of the time reversal Hamiltonian can be divided into two subspaces which can be called as even and odd depending on the relation between the vectors

and their time reversal partners. In the even subspace the Hamiltonian transforms under the time reversal operator as $H_k = \Theta H_k \Theta^{-1}$ and therefore the eigenvectors have this property that the $\Theta|v_i>$ is equivalent to $|v_i>$ up to a $U(2)$ rotation, here i is the band index. The four special points in half of the 2-D Brillouin zone which are time reversal invariant points belong to even subspace.

The eigenfunctions $|v_i>$ are orthogonal to their time reversal partner $\Theta|v_i>$ in odd subspace. The zeros of the Pfaffian $(Pf(\vec{k}))$ for the overlap matrix elements $\omega_{ij} =< v_i|\Theta|v_j >$ of the time reversal operator is related to the topological characteristic of the Hamiltonian. $|Pf(\vec{k})|$ vanishes in the odd space whereas in the even subspace is equal to 1 up to a $U(2)$ rotation. The Pfaffian of a skew symmetric matrix $\omega_{2\times 2}$ is its ω_{12} element and it has more complicated form for higher number of bands. Therefore the task of finding the topological characteristic of the Hamiltonain reduces to finding the complex zeros of the Pfaffian. The zeros can occur either in pairs of points in the Brillouin zone or on the lines depending on the symmetry of the system. Odd number of pairs of complex zeros or odd number of two times cutting the line of zeros as we go through half the Brillouin zone, indicates that we have non trivial topological insulator and even is the sign of trivial insulator [5].

In order to find the zeros of Pfaffian for the bichromatic lattice we plot directly the absolute value of the Pfaffian. Since the numerical diagonalization of the Hamiltonian do not return in general the wave functions with the time reversal invariance, we impose this constraint in the special points of the Brillouin zone using the following relation:

$$|v_i(k)>= \Theta|v_{i-1}(k)> . \tag{4.6}$$

The Pfaffian for lowest two bands of the band structure in Fig. 4.2a is shown in Fig. 4.3a. In the absence of the bichromatic lattice, the zeros of Pfaffian $|Pf(k)|$ occur along a line as shown in Fig. 4.3a. For the case when $V' = 0.5V$ and $V'' = 0.5V$, the system holds its nontrivial topology Fig. 4.3b when we consider two lowest twofold degenerate bands Fig. 4.2b of Hamiltonian Eq. (3.1). On the other hand for the case $V' = 0.5V$ and $V'' = 0.5V$ since we break the half translational symmetry of

the Hamiltonian Eq. (3.1) [6], there is a gap opening between the first and second band Fig. 4.2c which allows us to discuss the topological characteristics of the lowest band as well. The line of zero vanishes for the lowest band , which means that we have trivial insulator Fig. 4.3c. However the lowest two bands together still keep their non-trivial characteristic and we saw similar pattern as in Fig. 4.3b for this case. The lowest band for the case $V' = 0.5V$ and $V'' = 0$ is also trivial but the gap between the lowest bands is very narrow in Fig. 4.2b.

In order to implement the bichromatic optical lattice configuration experimentally, the standing wave generated by two laser beams of wavelength λ and wave vector $\vec{k_1}$ are superimposed to two other laser beams which are rotated by 60° relative to the axis of lattice, as shown in Fig. 4.4. The same method needed to be applied for the other direction along $\vec{k_2}$. The wave vector which is rotated relative to primary lattice configuration will have a component along the original wave vector $\vec{k_1}$ which for the angle 60° gives rise to the configuration Fig. 4.1b. There are other methods for implementing the bichromatic lattice but then the frequency of the lasers changes therefore not appropriate for the model we studied in this paper [40].

We considered the $\mathbb{Z}_2$ topological insulator of ultracold atomic system on a triangular optical lattice, introduced in Ref. [6], deformed globally by bichromatic potentials. We examined the effect of this deformation which can be as large as the insulating gap, on the topological character of the system. We found that the system retains its topological character robustly against this kind of perturbation for two lowest twofold degenerate bands. However the lowest twofold degenerate band has trivial topology. The large insulating gap of such topological bichromatic insulators with deep bichromatic deformation can be used for disorder and relativistic dynamics studies in the nearly free electron regime.

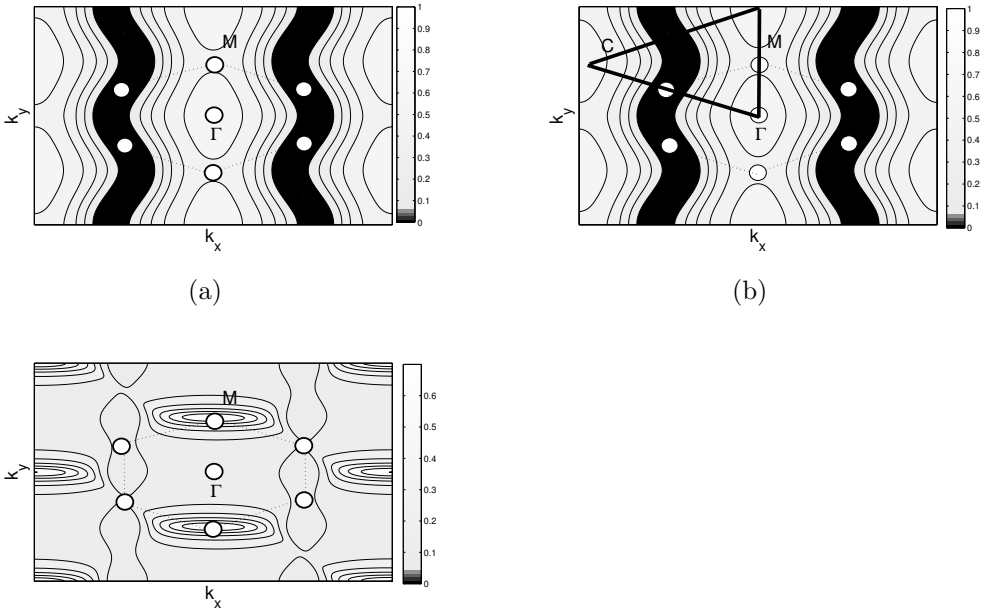

(a) (b)

(c)

Figure 4.3: The Pfaffian $|Pf(\vec{k})|$ in $\vec{k}$-space for different potentials in Eq. (4.6). Γ and M are high symmetry points. (a) $V' = 0$ and $V'' = 0$ are used to calculate the $|Pf(\vec{k})|$ of the the lowest twofold degenerate two bands. (b) $|Pf(\vec{k})|$ for $V' = 0.5V$ and $V'' = 0$. As one goes along the path C which includes the half of the first Brillouin zone one cut the line of zeros of $|Pf(\vec{k})|$ twice. This shows that system is still in non trivial topological state, which is the case for Fig. 4.3a as well. (c) $|Pf(\vec{k})|$ for lowest 2 bands for $V' = 0.5V$ and $V'' = 0.5V$ where there is no line of zeros therefore the system has trivial topology.

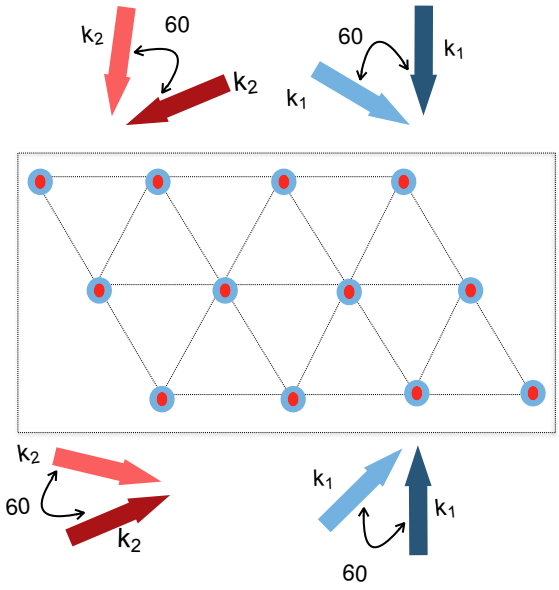

Figure 4.4: A schematic view of the bichromatic optical lattice which can be realised experimentally by using the standing waves generated by four laser beams of wavelength λ and wave vector $\vec{k_1}$ and $\vec{k_2}$, to which four other laser beams which are rotated by 60° relative to the axis of lattice are applied. The dark red and blue arrows refer to primary lattice laser field and the light colored red and blue arrows show the direction of the laser which superimpose the primary lattice. The blue colour circles are the lattice sites and red coloured circles are the bumps which the cross section view of them is shown in Fig.4.1b.

Chapter 5

A TIGHT BINDING MODEL FOR QUANTUM SPIN HALL EFFECT ON TRIANGULAR OPTICAL LATTICES

5.1 Introduction

Topological insulators (TIs) are insulating in the bulk but have metallic states on their boundaries [13, 15]. Robustness of these states against disorder and perturbations makes them promising for applications such as spintronics [14] and topological quantum computation [30]. Topological invariants of the bulk material are essential for the robust boundary modes. This urged consideration of topological insulators on different lattice geometries [31–35].

It is widely acknowledged that the cold atomic systems are ideal systems to simulate solid-state phenomena in a controlled way. The two and three dimensional topological insulators with band gaps in the order of the recoil energy have recently been proposed in ultracold fermionic atomic gases held in optical flux lattices in nearly free electron regime [6]. The proposal utilizes interactions which preserves time reversal symmetry (TRS), analogous to synthesized spin-orbit coupling [20], so that the insulators are classified by the so called $\mathbb{Z}_2$ topological invariant [21]. Optical lattices with different geometries can be experimentally generated, such as triangular, square, honeycomb and Kagome lattice. The physics of the triangular lattice has remarkable unique properties in frustration, spin chirality, quantum phase transition, spin liquids and quantum Hall effect. In the cold atomic systems there are many proposals for the triangular or hexagonal lattices which in particular exhibit new and very rich phases e.g. super solidity [46], exotic superconducting states [47] and graphene-like physics [48]. $\mathbb{Z}_2$ topological insulators has been discussed recently. Here, we propose

a simple way to generate quantum spin Hall system in a triangular lattice.

TIs in ultra cold atomic systems have been studied vastly in tight binding regime (TB) [22,23]. Such theoretical studies can not be implemented with optical flux lattice systems as they are originally proposed to operate far from the TB regime [49]. The optical lattices on the other hand can be used as deep potentials. Alternatively the phase imprinting process modulating the optical lattices periodically in time is a broadly applicable means for generating high flux gauge fields [50–52], which is a low demanding method. Implementing non-Abelian gauge fields are also done using this scheme [53].

Our aim in this article is to propose a tight binding model for the quantum spin Hall effect on triangular optical lattice without spin flip *i.e.* spin orbit coupling is proportional to σ_z. The advantage of the method that we use here is the lower spontaneous emission in comparison to the other methods which use spin-flip Raman process to create non-Abelian gauge fields. The reason is that the Rabi frequency and the spontaneous emission rate of two-photon Raman process with spin flip are proportional to the ratio of laser power to detuning which in the case of interacting systems requires longer lifetime due to smaller energy scale [51]. We also determine the band structure of the edge state which exhibits the hallmark of TIs due to its robustness against all perturbations that preserve the TRS .

In the Sec. 5.2 of this paper we propose the tight binding model for quantum spin Hall (QSH) system in the triangular optical lattice. In Sec. 5.3 we explain how to implement our model in experiment.

5.2 Tight Binding model

5.2.1 Bulk band structure

The charge quantum Hall effect depends on the breaking of time-reversal symmetry and it has been shown that even in the absence of average non-zero external magnetic field the quantum Hall effect can be created [3]. However in the QSH effect one needs to preserve the time reversal invariance. Among the first models proposed for

dissipationless QSH effect are the works by Bernevig and Zhang [4] and by Kane and Mele [5], where the authors used the spin-orbit coupling such that the two different spin direction experiences the same magnetic field strength but with opposite sign. In other words their system were two copies of a quantum Hall system for each spin where the total first Chern number adds up to zero and the system is time reversal invariant.

Physically our model corresponds to the same scenario. We propose a Hamiltonian for a fermion on triangular lattice Fig. 5.1 with a mirror symmetric spin orbit coupling as,

$$H = \sum_{m,n} t_1 C^{\dagger}_{m+1,n} \mathrm{e}^{i\phi_{m,n}\sigma_z} C_{m,n} + t_2 C^{\dagger}_{m,n+1} C_{m,n} + t_{12} C^{\dagger}_{m+1,n+1} \mathrm{e}^{i\phi'_{m,n}} \sigma_z C_{m,n} + H.c.. \tag{5.1}$$

Where $\phi = \pi n$ and $\phi' = (2n+1)\pi/2$. The resulting flux per plaquette is $1/4$. $C_{m,n} = (c_{m,n\uparrow}, c_{m,n\downarrow})^T$ and $C^{\dagger}_{m,n}$ are annihilation and creation operators on site (m,n) respectively. We take the hopping parameter along the $\vec{a}_1$, $\vec{a}_2$ and diagonal on the triangular lattice with $\vec{a}_1 = (\sqrt{3}/2, -1/2)a$ and $\vec{a}_2 = (0,1)a$, where a is

the lattice constant (see Fig. 5.1). Which is taken to be $t_1 = t_2 = t_{12}$ correspondingly which we take them to be equal to t throughout this paper. The first term is nearest neighbour hopping term The second and third terms are mirror symmetric spin-orbit interaction. σ_z is the Pauli matrix. In the absence of spin this Hamiltonian implies that electron acquires $\phi = 1/4$ of flux quantum enclosing the elementary plaquette of the triangular lattice. This Hamiltonian is invariant under the time reversal operator,

$$T = i\sigma_y \otimes \mathbb{1}. \tag{5.2}$$

In order to calculate the band structure we take the Fourier transform of the

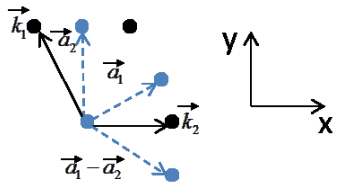

Figure 5.1: The light points and dashed lines show the lattice sites of the atoms and the hopping directions in the triangular lattice respectively, and the dark points and lines are the corresponding Brillouin zone sites and vectors respectively.

Hamiltonian Eq. (5.1). We use the momentum representation of fermionic operator

$$C_{\mathbf{k}} = \sum_{m,n} e^{i\mathbf{k}\cdot\mathbf{R}_{m,n}} C_{m,n}, \tag{5.3}$$

where $\mathbf{R}_{m,n} = m\vec{a}_1 + n\vec{a}_2$. We obtain the energy dispersion in triangular lattice by solving the determinant for the eigenvalues ϵ,

$$\mathrm{Det}\begin{bmatrix} A-\epsilon & B+iC & 0 & 0 \\ B-iC & -A-\epsilon & 0 & 0 \\ 0 & 0 & A-\epsilon & B-iC \\ 0 & 0 & B+iC & -A-\epsilon \end{bmatrix} = 0, \tag{5.4}$$

where A,B and C are defined to be,

$$A = t_2 \cos\left(k_y a\right), \tag{5.5}$$

$$B = t_1 \cos\frac{a}{2}\left(\sqrt{3}k_x - k_y\right), \tag{5.6}$$

$$C = t_{12} \cos\frac{a}{2}\left(\sqrt{3}k_x + k_y\right). \tag{5.7}$$

In order to solve Eq. (5.4), we used a 2D grid for the $\vec{k}$-space. Fig. 5.2a shows the band structure of the Eq. (5.4) for a cell with specific $\vec{k}$ points as its corners taken to be $(\kappa_1 + \kappa_2)/2$, $\kappa_1/2$, 0, $\kappa_2/2$, as shown in the inset. These points are the TRS invariant points in the Brillouin zone Since each of the two blocks of the Eq. (5.4) corresponds to two fold spin degenerate bands, each band of the Fig. 5.2a is four fold degenerate.

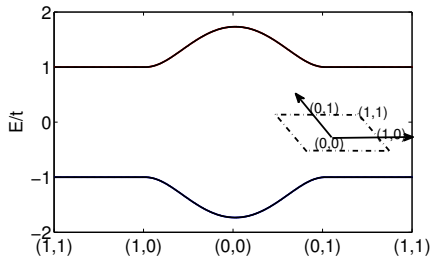

(a)

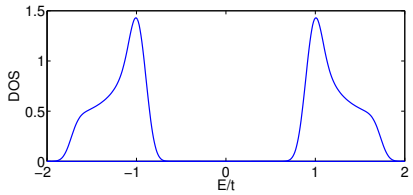

(b)

Figure 5.2: (a) The band structure of the Hamiltonian Eq. (5.1) along the path (1,1), (1,0), (0,0), (0,1) where 1 and 0 are referring to the inset (m,n) in $\vec{\Gamma}_{mn} = (m\vec{\kappa}_1 + n\vec{\kappa}_2)$, which are the TRS invariant points in Brillouin zone. The bands are four fold degenerate as in the nearly free electron limit of cold atomic system. (b) The DOS for all the energy bands is shown where the horizontal axis is the energy.

We also calculated the density of states (DOS) for the Hamiltonian in Eq. (5.4). This quantity is defined by the expression,

$$\rho(E) = \frac{1}{A}\sum_{\mathbf{k}} \delta(E - E_n), \tag{5.8}$$

where A is the area of the system in reciprocal space and E_n is the energy of the bands. In Fig. 5.2b the DOS is depicted for all the energy bands.

5.2.2 Edge-state band structure

The characteristic of the $\mathbb{Z}_2$ topological insulator is the gapless edge states. They describe two spin currents at the edge, propagating in opposite direction. This property is because of the the time-reversal symmetry and it prevents the gap opening due to

any TR invariant perturbation as the result of the Kramer's theorem [5].

We follow the method in Ref. [54] to find the energy dispersion of the edge states. The Hamiltonian Eq. (5.1), must be reduced to a one-dimensional problem. We take the y direction as the periodic part and we use the momentum representation as,

$$C_{m,n} = \frac{1}{\sqrt{L_x}} \sum_{k_x} e^{ik_x m} C_n(k_x), \tag{5.9}$$

where $k_x a/2 = 2\pi m_x/L_x$, $m_x = 1, ..., L_x$ and L_x is the system size along x direction. By inserting the single particle state

$$|\Psi(k_x)\rangle = \sum_n |\Psi_n(k_x)\rangle C_n^\dagger(k_x)|0\rangle \tag{5.10}$$

into the Schrödinger equation $H|\Psi\rangle = E|\Psi\rangle$, the spin up part of the problem is reduced to the one-dimensional problem with parameter k_y as

$$\begin{aligned} G'\Psi_{n+1} - G\Psi_{n-1} - 2\cos\left(k_x a/2 - 4\pi\phi n\right)\Psi_n \\ = E\psi_n. \end{aligned} \tag{5.11}$$

where $G = 1 + e^{i(k_x a/2 + \pi\phi(2n-1))}$ and $G' = 1 + e^{-i(k_x a/2 + \pi\phi(2n+1))}$. Including the spin down as well, this equation can be written as a generalized Harper equation [55] ,

$$\begin{pmatrix} \Psi_{1\uparrow}(k_x) \\ \Psi_{2\uparrow}(k_x) \\ . \\ . \\ . \\ \Psi_{N\uparrow}(k_x) \\ \Psi_{1\downarrow}(k_x) \\ \Psi_{2\downarrow}(k_x) \\ . \\ . \\ . \\ \Psi_{N\downarrow}(k_x) \end{pmatrix} = M \begin{pmatrix} \Psi_{1\uparrow}(k_x) \\ \Psi_{2\uparrow}(k_x) \\ . \\ . \\ . \\ \Psi_{N\uparrow}(k_x) \\ \Psi_{1\downarrow}(k_x) \\ \Psi_{2\downarrow}(k_x) \\ . \\ . \\ . \\ \Psi_{N\downarrow}(k_x) \end{pmatrix}, \tag{5.12}$$

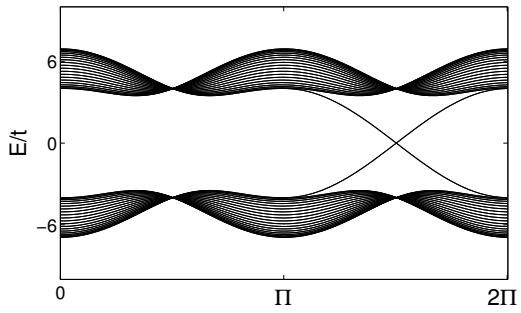

Figure 5.3: The spectrum of the edges of triangular lattice. The shaded area is lowest energy bands for the triangular lattice. The solid lines show the spin polarized edge state band, traversing the gap. The edge states cross at $k_y a = 3\pi/2$

where M is the transfer matrix, which is given by:

$$M = \begin{pmatrix} F_1 & G_1 & 0 & \dots & 0 & 0 & 0 & 0 \\ G_1' & F_2 & G_2 & \dots & 0 & 0 & 0 & 0 \\ 0 & \vdots & \ddots & \ddots & \ddots & 0 & 0 & 0 \\ 0 & 0 & G_{N-1}' & F_N & G_N & & & \\ 0 & 0 & 0 & F_1 & R_1 & \dots & 0 & 0 \\ 0 & 0 & 0 & R_1' & F_2 & R_2 & \dots & 0 \\ 0 & 0 & 0 & 0 & 0 & \ddots & \ddots & \ddots \\ 0 & 0 & 0 & 0 & 0 & 0 & R_{N-1}' & F_N \end{pmatrix} \tag{5.13}$$

with $R = 1 - e^{i(k_x a/2 + \pi\phi(2n-1))}$, $R' = 1 - e^{-i(k_x a/2 + \pi\phi(2n+1))}$ and $F = -\epsilon - 2\cos(k_x a/2 - 4\pi\phi n)$. Under the boundary condition that the wavefunction goes to zero at the boundaries of lattice we can solve this equation. The band structure along the path $k_y a = 0 - 2\pi$ is shown in the Fig. 5.3. We used 100 k-points along k_y direction. The shaded area is the bulk band.

5.3 Cold Atomic system

The Hamiltonian of a noninteracting particle on a 2D lattice can be written as

$$\begin{aligned} H &= \sum_{m,n} -\frac{J_1}{2} C^{\dagger}_{m,n+1} C_{m,n} + h.c. \\ &\quad -\frac{J_2}{2} C^{\dagger}_{m+1,n} C_{m,n} + h.c. \\ &\quad -\frac{J_{12}}{2} C^{\dagger}_{m+1,n+1} C_{m,n} + h.c. + \\ &\quad \frac{a}{2}[mF + F_\omega \cos(\omega t + \phi)] C^{\dagger}_{m,n} C_{m,n}, \end{aligned} \tag{5.14}$$

where $C_{m,n}$ and $C^{\dagger}_{m,n}$ are annihilation and creation operators respectively, and a is the lattice constant. J_1, J_2, J_{12} are the hopping parameters along the lattice vectors $\vec{a}_1$, $\vec{a}_2$, $\vec{a}_1 + \vec{a}_2$ respectively. This is the Hamiltonian of optical lattice that is tilted and driven along $\hat{x}$ direction with AC and DC amplitude, F_ω and F respectively and is basically a triangular lattice. The Bloch oscillation frequency is $af/2h$ and ϕ is an arbitrary phase which we use to create magnetic field using Raman beams.The DC part can be created by gravity or magnetic field gradients and the AC part can be created using Raman beams [55]. In the absence of external constant or time-periodic forces, the eigenfunctions of the Hamiltonian Eq. (5.14) are Wannier functions but in the presence of the AC and DC fields the eigenfunctions are Wannier-Stark type [56].

The operator of the unitary transformation to a rotating frame follows as,

$$U = \exp[\sum_{m,n} i \left(m\omega t + \frac{F_\omega}{\hbar\omega} \left(\sin\left(\omega t + \phi_{m,n}\right)\right)\right) C^{\dagger}_{m,n} C_{m,n}] = \sum_{m,n} e^{i\gamma_{m,n} C^{\dagger}_{m,n} C_{m,n}} \tag{5.15}$$

where $\gamma_{m,n} = m\omega t + \frac{F_\omega}{\hbar\omega}\left(\sin\left(\omega t + \phi_{m,n}\right)\right)$. After applying the relation $H' = UHU^{\dagger} - i\hbar \dot{U}^{\dagger} U$ and taking $\hbar\omega = aF/2$, one gets the following coefficients for the hopping terms in the Hamiltonian Eq. (5.14) J_1, J_2 and J_{12} respectively,

$$\exp[-i\left(\gamma_{m,n+1} - \gamma_{m,n}\right)] = \exp[-i\frac{F_\omega}{\hbar\omega}\left(\cos(\omega t + \phi_{m,n+1}) - \cos(\omega t + \phi_{m,n})\right)] \tag{5.16}$$

$$\exp[-i\left(\gamma_{m+1,n} - \gamma_{m,n}\right)] = \exp[-i\left(\omega t + \frac{F_\omega}{\hbar\omega}\left(\cos(\omega t + \phi_{m+1,n}) - \cos(\omega t + \phi_{m,n})\right)\right)]$$

$$\exp[-i\left(\gamma_{m+1,n+1} - \gamma_{m,n}\right)] = \exp[-i\left(\omega t + \frac{F_\omega}{\hbar\omega}\left(\cos(\omega t + \phi_{m+1,n+1}) - \cos(\omega t + \phi_{m,n})\right)\right)].$$

Using the relations $\cos A - \cos B = -2\sin(A+B)/2\sin(A-B)/2$ and $exp(ix\sin\theta) = \sum_r j_r(x)\exp(irt)$ one can simplify the equations further to obtain the following terms,

$$\begin{aligned}
\mathrm{e}^{-i(\gamma_{m,n+1}-\gamma_{m,n})} &= \sum_{r=-\infty}^{\infty} j_r\left(\frac{\sin(\frac{\mathbf{k}\cdot\mathbf{a}_2}{2})F_\omega}{\hbar\omega}\right)\mathrm{e}^{ir\left(\omega t+\vec{k}\cdot\frac{\vec{a}_2}{2}\right)+\phi_{m,n}} \qquad (5.17)\\
\mathrm{e}^{-i(\gamma_{m+1,n}-\gamma_{m,n})} &= \mathrm{e}^{-i\omega t}\sum_{r=-\infty}^{\infty} j_r\left(\frac{\sin(\frac{\mathbf{k}\cdot\mathbf{a}_1}{2})F_\omega}{\hbar\omega}\right)\mathrm{e}^{ir\omega t+\vec{k}\cdot\frac{\vec{a}_1}{2}+\phi_{m,n}}\\
\mathrm{e}^{-i(\gamma_{m+1,n+1}-\gamma_{m,n})} &= \mathrm{e}^{-i\omega t}\sum_{r=-\infty}^{\infty} j_r\left(\frac{\sin(\frac{\mathbf{k}\cdot(\mathbf{a}_1+\mathbf{a}_2)}{2})F_\omega}{\hbar\omega}\right)\times\\
&\quad \mathrm{e}^{ir\omega t+\vec{k}\cdot\frac{(\vec{a}_1+\vec{a}_2)}{2}+\phi_{m,n}}.
\end{aligned}$$

Taking the average over one period of time $\tau \sim 1/\omega$ for the J_1 leaves us only with $r = 0$ option however the other terms (J_2 and J_{12}) will be changed. Then we can write the effective Hamiltonian as,

$$\begin{aligned}
H &= \sum_{m,n} -\frac{J_1}{2}C^\dagger_{m,n+1}C_{m,n} + h.c.\\
&\quad -\frac{\widetilde{J}_2}{2}C^\dagger_{m+1,n}e^{i\left(\phi_{m,n}+\frac{\mathbf{k}\cdot\mathbf{a}_1}{2}\right)}C_{m,n} + h.c.\\
&\quad -\frac{\widetilde{J}_{12}}{2}C^\dagger_{m+1,n+1}C_{m,n}e^{i\phi'_{m,n}} + h.c.. \qquad (5.18)
\end{aligned}$$

where,

$$\begin{aligned}
\widetilde{J}_2 &= j_1(\frac{\sin(\frac{\mathbf{k}\cdot\mathbf{a}_1}{2})F_\omega}{\hbar\omega})J_2,\\
\widetilde{J}_{12} &= j_1(\frac{\sin(\frac{\mathbf{k}\cdot(\mathbf{a}_1+\mathbf{a}_2)}{2})F_\omega}{\hbar\omega})J_{12}. \qquad (5.19)
\end{aligned}$$

Here j_1 is the Bessel function of the first kind. Since we are interested in quantum spin Hall we need to incorporate spin into our system this can be done using the Raman transitions in optical lattice. The phase ϕ can be generated by $\vec{k}\cdot R_{m,n}$ where $\vec{k} = \vec{k}_1 - \vec{k}_2$ which is the momentum transferred from two far-detuned Raman beams of two-photon Rabi frequency Ω. $\phi_{m,n} = m\vec{k}\cdot\vec{a_1} + n\vec{k}\cdot\vec{a}_2$ and $\phi'_{m,n} = (m+1/2)\vec{k}\cdot\vec{a}_1 + (n+1/2)\vec{k}\cdot\vec{a}_2$ is the momentum transfer of the Raman lasers [50]. Additionally if we take the states of the same hyperfine level and opposite magnetic quantum number M_F,

we can reverse the process of laser beams absorption of a photon versus stimulated emission of a photon for the Raman process in a way that the two states receive opposite momentum transfer. This means that the opposite spin direction accumulate different sign of phase encircling a plaquette in the unit cell. The Hamiltonian Eq. (5.18) now can be written as,

$$\begin{aligned} H &= \sum_{m,n} -\frac{J_1}{2} C^{\dagger}_{m,n+1} C_{m,n} + h.c. \\ &\quad -\frac{\widetilde{J}_2}{2} C^{\dagger}_{m+1,n} e^{i\phi_{m,n}\sigma_z} C_{m,n} + h.c. \\ &\quad -\frac{\widetilde{J}_{12}}{2} C^{\dagger}_{m+1,n+1} C_{m,n} \times \\ &\quad e^{i(\phi_{m,n}+(\vec{a}_1+\vec{a}_2)\frac{k}{2}\sigma_z} + h.c.. \end{aligned} \tag{5.20}$$

In order to make the flux 1/4 which makes the Hamiltonian in Eq.(5.1) and Eq. (5.20) identical one needs to choose $\vec{k}\cdot\vec{a}_1 = 4\pi$ and $\vec{k}\cdot\vec{a}_2 = \pi$ and use the identity $e^{i\theta\sigma_z} = \cos(\theta)\mathbb{1} + \sin(\theta)\sigma_z$.

Summarising, we proposed a quantum spin Hall model on a triangular lattice in the tight-binding limit which can be realized in an ultra cold atomic system using tilted optical lattices driven by two-colour and Raman lasers. We studied the edge state band structure to verify the $\mathbb{Z}_2$ character of the system.

Chapter 6

CONCLUSION AND OUTLOOK

In the present work, we studied the realisation of $\mathbb{Z}_2$ topological insulators on optical lattices. We specifically studied triangular lattice systems, since in the cold atomic systems there are many proposals for triangular or hexagonal lattices which in particular exhibit new and very rich phases such as super solidity [46], exotic superconducting states [47] or graphene-like physics [48]. In order to implement spin-orbit coupling on neutral atoms we used two main methods. First method is given by Beri and Cooper [6] which was originally given in the nearly free electron limit and we studied it in deep potential limit which is the regime of tight-binding systems. The importance of the tight-binding regime is that we can use such models to study new aspects like introducing interaction into system and study possible new topological phases which can be implemented experimentally as well.

Next we discussed the effect of introducing a global perturbation to the $\mathbb{Z}_2$ topological insulator. We know that a local perturbation doesn't break the topological phase of a system. We tried to answer these questions for a global perturbation by studying topological insulators on a bichromatic triangular lattice. In order to study the topological phases we used the Pfaffian method introduced in Ref. [5]. We found out that for perturbations which do not change the lattice configuration, the topology of a half filled system can not be broken but the degeneracy at highly symmetric points in k-space can be lifted for two first double degenerate bands the degeneracy is lifted and the states which are filled in the first double degenerate band become topologically trivial.

Finally we used another method to create a quantum spin Hall system, which is based on shaking optical lattices. It can be shown that the application of AC and

DC fields imprint phase on atoms while hopping. The phase can be tuned using the wave vectors of Raman lasers to create an artificial gauge field. We used this method to study the quantum spin Hall effect on triangular systems. We studied the edge states which are the hall mark of topologicaly non-trivial phases. This method can be generalised to hexagonal system, and also to interacting systems.

6.1 Outlook

In this work, the $\mathbb{Z}_2$ topological insulators for non interacting single Hamiltonian on a triangular optical lattice is studied. An immediate extension of this work is to introduce interactions to the system. The advantage of cold atoms on optical lattices is that these systems are highly tuneable and one can control the interactions between atoms in an impurity free environment. This may be achieved in the lab by tuning the interaction, using the Feshbach resonance.

BIBLIOGRAPHY

[1] F. Gerbier and J. Dalibard. *New Jour. Phys.*, 12:033007, 2010.

[2] D. J. Thouless, M Kohmoto, M. P. Nightingale, and M. den Nijs. *Phys. Rev. Lett*, 49:405, 1982.

[3] F. D. M. Haldane. *Phys. Rev. Lett*, 61:2015, 1988.

[4] B. Andrei Bernevig and Shou-Cheng Zhang. *Phys. Rev. Lett.*, 96:106802, 2006.

[5] C.L. Kane and E.J. Mele. *Phys. Rev. Lett.*, 95:146802, 2005.

[6] B. Béri and N. R. Cooper. *Phys. Rev. Lett.*, 107:145301, 2011.

[7] A. K. Ardabili, T. Dereli, and Ö. Müstecaplioğlu. *Physica B*, 451:1, 2015.

[8] A. K. Ardabili, T. Dereli, and Ö. Müstecaplioğlu. *A Tight Binding Model for Quantum Spin Hall Effect on Triangular Optical Lattices. arXiv:1401.3179.*

[9] A. K. Ardabili, T. Dereli, and Ö. Müstecaplioğlu. *A Tight Binding Model for Quantum Spin Hall Effect Using Laser-Assisted Tunneling on Triangular Optical Lattices. Submitted to Modern Physics Letters B.*

[10] M. Kohmoto. *Annals of Physics*, 160:343, 1985.

[11] M. Nakahara. *Geometry, Topology and Physics, Second Edition.* CRC Press, 2003.

[12] S. Ryu, C. Mudry, H. Obuse, and A. Furusaki. *Phys. Rev. Lett.*, 99:116601, 2007.

[13] M. Z. Hasan and C. L. Kane. *Rev. Mod. Phys.*, 82:3045, 2010.

[14] J. E. Moore. *Nature*, 464:194, 2010.

[15] X. L. Qi and S. C. Zhang. *Rev. Mod. Phys.*, 83:1057, 2011.

[16] T. Fukui and Y. Hatsugai. *J. Phys. Soc. Japan.* , 76:053702, 2007.

[17] J.D.Jackson. *Classical Electrodynamics*. John Wiley & Sons, 1998.

[18] C. Cohen-Tannoudji, J. Dupont-Roc, and G. Grynberg. *Atom-Photon Interactions*. Wiley, New York, 1992.

[19] R. Grimm, M. Weidemuller, and Yu.B. Ovchinnikov. *Adv. At. Mol. Opt. Phys.*, 42:95, 2000.

[20] Y.-J. Lin, K. Jiménez-García, and I. B. Spielman. *Nature*, 471:83, 2011.

[21] L. Fu and C. L. Kane. *Phys. Rev. B*, 74:195312, 2006.

[22] G. Juzeliunas, J. Ruseckas, and J. Dalibard. *Phys. Rev. A*, 81:053403, 2010.

[23] N. Goldman, I. Satija, P. Nikolic, A. Bermudez, M. A. Martin-Delgado, M. Lewenstein, and I. B. Spielman. *Phys. Rev. Lett.*, 105:255302, 2010.

[24] S. Murakami, N. Nagaosa, and S.C. Zhang. *Science*, 301:1348, 2003.

[25] J. Dalibard, F. Gerbier, G. Juzeliunas, and P. Öhberg. *Rev. Mod. Phys.*, 83:1523, 2011.

[26] D. Jaksch and P. Zoller. *Annals of Physics*, 315:52, 2005.

[27] Charles Kittel. *Introduction to Solid State Physics*. John Wiley & Sons, 2005.

[28] D. Jaksch, C. Bruder, J. I. Cirac, C. W. Gardiner, and P. Zoller. *Phys. Rev. Lett*, 81:3108, 1998.

[29] N. W. Ashcroft and N. David Mermin. *Solid State Physics*. Thomson Learning, Toronto, 1976.

[30] C. Nayak, S. H. Simon, A. Stern, M. Freedman, , and S. Das Sarma. *Rev. Mod. Phys.*, 80:1083, 2008.

[31] X. Hu, M. Kargarian, and G. A. Fiete. *Phys. Rev. B*, 84:155116, 2011.

[32] C. Weeks and M. Franz. *Phys. Rev. B*, 82:085310, 2010.

[33] H.-M. Guo and M. Franz. *Phys. Rev. B*, 80:113102, 2009.

[34] H.-M. Guo and M. Franz. *Phys. Rev. Lett.*, 103:20680, 2009.

[35] L. Fu, C. L. Kane, and E. J. Mele. *Phys. Rev. Lett.*, 98:106803, 2007.

[36] G. Schubert, H Fehske, L. Fritz, and M. Vojta. *Phys. Rev. B.*, 85:201105, 2012.

[37] D. Witthaut, T. Salger, S. Kling, C. Grossert, and M. Weitz. *Phys. Rev. A*, 84:033601, 2011.

[38] L. Mazza, N. Goldman A. Bermudez, M. Rizzi, M. A Martin-Delgado, and M. Lewenstein. *New Jour. Phys.*, 14:015007, 2012.

[39] S. Aubry and G. André. *Ann. Israel Phys. Soc.*, 3:133, 1980.

[40] G. Roati, C. D'Errico, L. Fallani, M. Fattori, C. Fort, M. Zaccanti, G. Modugno, M. Modugno, and M. Inguscio. *Nature*, 453:895898, 2008.

[41] B. Deissler, M. Zaccanti, G. Roati, C. DErrico, M. Fattori, M. Modugno, G. Modugno, and M. Inguscio. *Nature Phys.*, 6:354, 2010.

[42] F. Mei, S.-L. Zhu, A.-M. Zhang, C. H. Oh, and N. Goldman. *Phys. Rev. A*, 85:013638, 2012.

[43] L.-J. Lang, X. Cai, and S. Chen. *Phys. Rev. Lett.*, 108:220401, 2012.

[44] L. D. Landau and E. M. Lifshitz. *Quantum Mechanics*. Pergamon, London, 1958.

[45] R. Roy. *Phys. Rev. B*, 79:195321, 2009.

[46] S. Wessel and M. Troyer. *Phys. Rev. Lett*, 95:127205, 2005.

[47] L. Mathey, S. W. Tsai, and A. H. Neto. *Phys. Rev. B*, 97:190406, 2006.

[48] G. Juzeliunas, J. Ruseckas, M. Lindberg, and M. Öhberg. *Phys. Rev. A*, 77:011802, 2008.

[49] N. R. Cooper and R. Moessner. *Phys. Rev. Lett*, 109:215302, 2012.

[50] J. Struck, M. Weinberg, C. Öschläger, P. Windpassinger, J. Simonet, K. Sengstock, R. Höppner, P. Hauke, A. Eckardt, M. Lewenstein, and L. Mathey. *Nature Physics*, 9:738, 2013.

[51] C. J. Kennedy, G. A. Siviloglu, H. Miyake, W. C. Burton, and W. Ketterle. *Phys. Rev. Lett*, 111:225301, 2013.

[52] J. Struck, C. Öschläger, M. Weinberg, P. Hauke, J. Simonet, A. Eckardt, M. Lewenstein, K. Sengstock, and P. Windpassinger. *Phys. Rev. Lett*, 108:225304, 2012.

[53] Philipp Hauke, Olivier Tieleman, Alessio Celi, ChristophÖolschläger, Juliette Simonet, Julian Struck, Malte Weinberg, Patrick Windpassinger, Klaus Sengstock, Maciej Lewenstein, and Andre Eckardt. *Phys. Rev. Lett*, 109:145301, 2012.

[54] Y. Hatsugai. *Phys. Rev. B*, 48:11851, 1993.

[55] P. G. Harper. *Proc. Phys. Soc. A*, 68:874, 1955.

[56] F. Keck and H. J. Korsch. *Phys. Rev. Lett*, 61:2015, 1988.